Gene expression profiling of granule cells and Purkinje cells in the zebrafish cerebellum

Miki Takeuchi[1], Shingo Yamaguchi[2], Masayoshi Sakakibara[2], Takuto Hayashi[2], Koji Matsuda[1,2], Yuichiro Hara[3], Chiharu Tanegashima[3], Takashi Shimizu[1,2], Shigehiro Kuraku[3], Masahiko Hibi[1,2]

[1]Laboratory of Organogenesis and Organ Function, Bioscience and Biotechnology, Nagoya University, Nagoya, Aichi 464-8602, Japan
[2]Division of Biological Science, Graduate School of Science, Nagoya University, Nagoya, Aichi 464-8602, Japan
[3]RIKEN Center for Life Science Technologies, Kobe, Hyogo 650-0047, Japan

Abbreviated Title: Transcriptomes in zebrafish cerebellar neurons

Key words: RNA-seq, cerebellar gene enrichment, cerebellum-like structures, RRID:ZIRC_ZL1, RRID: AB_10013361, RRID: SCR_001370, RRID: SCR_001120

Correspondence: Masahiko Hibi
Laboratory of Organogenesis and Organ Function, Bioscience and Biotechnology Center, Nagoya University, Furo, Chikusa, Nagoya 464-8601, Tel: +81-52-789-5198, Fax: +81-52-789-5053, E-mail: hibi@bio.nagoya-u.ac.jp

Footnote: Supported by Grants-in-Aid for Scientific Research (B and C) from the Ministry of Education, Science, Sports and Technology (MEXT), Japan (24370088 to M.H., 25440104 to T.S., and 16K18548 to M.T.); by Grants-in-Aid for Scientific Research on Innovative Areas from MEXT (25111709, 26115512 to M.H.); and by Takeda Science Foundation (to M.H.).

Abstract

The structure of the neural circuitry of the cerebellum, which functions in some types of motor learning and coordination, is generally conserved among vertebrates. However, some cerebellar features are species-specific. It is not clear which genes are involved in forming these conserved and species-specific structures and functions. Here, using zebrafish transgenic larvae expressing fluorescent proteins in granule cells, Purkinje cells, or other cerebellar neurons and glial cells, we isolated each type of cerebellar cells by fluorescence-activated cell sorting and profiled their gene expressions by RNA sequencing and *in situ* hybridization. We identified genes that were upregulated in granule cells or Purkinje cells, including many genes that are also expressed in mammalian cerebella. A comparison of the transcriptomes in granule cells and Purkinje cells in zebrafish larvae revealed that more developmental genes are expressed in granule cells, whereas more neuronal-function genes are expressed in Purkinje cells. We further found that some genes that are upregulated in granule cells or Purkinje cells are also expressed in the cerebellum-like structures. Our data provide a platform for understanding the development and function of the cerebellar neural circuits in zebrafish, and the evolution of cerebellar circuits in vertebrates.

Introduction

The cerebellum is active in some forms of motor learning and coordination, and is thought to function in higher cognitive and emotional functions (Ito, 2005; 2006; 2008). Cerebellar functions rely on neural circuits that are relatively conserved among vertebrates (Butler and Hodos, 1996). In all vertebrate species, the cerebellum contains similar sets of neurons and glial cells (Butler and Hodos, 1996; Altman and Bayer, 1997). The major glutamatergic excitatory and GABAergic inhibitory neurons in the cerebellum are the granule cells and Purkinje cells, respectively. Granule cells, which are derived from neuronal progenitors located in the upper rhombic lip, express the proneural gene *atoh1*, whereas Purkinje cells, which are derived from neuronal progenitors located in the ventricular zone, express the proneural gene *ptf1a* (Wingate and Hatten, 1999; Wingate, 2001; Zervas et al., 2004; Wingate, 2005; Hoshino, 2006). Although the two sets of neuronal progenitors are located in adjacent regions of the dorso-anterior hindbrain, they follow distinct genetic programs for their differentiation to granule or Purkinje cells.

Purkinje cells and granule cells receive afferent inputs from outside the cerebellum through climbing fibers and mossy fibers, respectively (Butler and Hodos, 1996; Altman and Bayer, 1997). Climbing fibers, which originate from the inferior olive nucleus (IO) in the caudoventral hindbrain, innervate the dendrites of Purkinje cells. Mossy fibers, which are the axons of neurons in the precerebellar nuclei found in various regions of the brain, form synapses with granule-cell dendrites. Information is conveyed from the mossy fibers to Purkinje-cell dendrites by the axons of the granule cells, which are called parallel fibers. Information from mossy fibers and climbing

fibers is integrated into the Purkinje cells, which send outputs to projection neurons that extend axons outside the cerebellum. The mammalian cerebellum, and the valvula cerebelli and the corpus cerebelli (the anteromedial lobes) of the teleost cerebellum have three layers (Butler and Hodos, 1996; Altman and Bayer, 1997; Bae et al., 2009; Hashimoto and Hibi, 2012; Hibi and Shimizu, 2012). Granule cells are in the deepest layer, called the granule-cell layer; Purkinje-cell somata are in the Purkinje-cell layer, which is above the granule-cell layer; and parallel fibers form synapses on the dendrites of Purkinje cells in the superficial layer, called the molecular layer. In addition to the cerebellar neurons, Bergmann glia cell bodies are located near the Purkinje-cell layer or in the molecular layer and extend glial processes to both the superficial (pial) and deep (ventricular) sides (Altman and Bayer, 1997; Bae et al., 2009).

Although essential structures of the cerebellum are conserved, comparative anatomical studies have revealed species-specific features (Butler and Hodos, 1996). In particular, the cerebella of zebrafish and other teleosts have features not seen in mammalian cerebella. For example, in the mammalian cerebellum, projection neurons are found in cerebellar nuclei deep inside the brain, while in the teleost cerebellum, the projection neurons (called eurydendroid cells) are located near the Purkinje cells (Nieuwenhuys et al., 1974; Finger, 1978; Pouwels, 1978; Ikenaga et al., 2005; 2006; Bae et al., 2009). The origin of projection neurons may also differ between mammals and zebrafish (Kani et al., 2010). Furthermore, the zebrafish caudolateral lobes (the lobus caudalis cerebelli and eminentia granularis) contain only granule cells (Bae et al., 2009). The granule cells in the anteromedial lobes send their axons only to the dendrites of Purkinje cells, whereas granule cells in the caudolateral lobes send axons to the

dendrites of Purkinje cells in the cerebellum, and further extend the axons to the dendrites of crest cells in the crista cerebellaris of the dorsal hindbrain (Bae et al., 2009; Volkmann et al., 2010; Wullimann and Grothe, 2014; Takeuchi et al., 2015b). As the neural circuits involving the crest cells in the dorsal hindbrain (the medial octavolateral nucleus: MON and the descending octaval nucleus: DON) and the marginal layer of the optic tectum have a neural-circuit structure similar to the cerebellum, they are called cerebellum-like structures (Bell, 2002; Bell et al., 2008; Hibi and Shimizu, 2012). The neurons in the cerebellum and cerebellum-like structures express a similar set of genes (Hibi and Shimizu, 2012). For instance, Purkinje cells, crest cells, and type I neurons (which are Purkinje-like cells in the optic tectum) express parvalbumin7, glutamate receptor delta2 (*grid2*), and retinoid-related orphan receptor alpha 2 (*rora2*) (Mikami et al., 2004; Katsuyama et al., 2007; Bae et al., 2009). It is not known whether the cerebellum-like structures share other patterns of gene expression. Furthermore, it is not clear which genes are involved in the formation of conserved and species-specific cerebellar structures and in the function of cerebellar neural circuits.

The molecular mechanisms of the development and function of the mammalian cerebellum have been investigated by transcriptome analysis (Schuller et al., 2006; Sato et al., 2008; Ha et al., 2015). Sato et al. generated a database of transcriptomes in the mouse cerebellum from embryonic and postnatal cerebella (Sato et al., 2008). Ha et al. studied cerebellar transcriptomes from mouse embryonic and postnatal cerebella (Ha et al., 2015). These studies were based on RNA collected from the whole cerebella, and might have missed minor but cell-type-specific genes. Schüller et al. (Schuller et al., 2006) focused on the expression profiles of genes encoding

transcription factors in the postnatal cerebellum; however, gene expression at the beginning of cerebellar neurogenesis remains to be elucidated. The data from these studies provide information about dynamic gene expression in the mammalian cerebellum, but must be compared with transcriptome data from the cerebella of other vertebrate species to elucidate the evolution and development of the cerebellum in vertebrates. The analysis of cell-type-specific transcriptomes will also add reliable information about rare genes that are expressed in differentiating neurons.

In zebrafish, the differentiation of granule cells and Purkinje cells is detected from the early larval stage (3 days post-fertilization, dpf), and simple cerebellar neural-circuit structures are observed by 5 dpf (Bae et al., 2009; Kani et al., 2010; Tanabe et al., 2010). Granule cells are generated continuously throughout the animal's life, and Purkinje cells are generated at the larval stage (through 30 dpf) (Zupanc et al., 2005; Kaslin et al., 2009; Kani et al., 2010; Kaslin et al., 2013). We have established zebrafish transgenic (Tg) lines that express modified Gal4 or fluorescent protein (or both) in the granule cells, Purkinje cells, eurydendroid cells, IO neurons, or Bergmann glial cells at the larval stage (Tanabe et al., 2010; Takeuchi et al., 2015a). Many of these Tg lines express the reporter protein from the early larval stage to adulthood (Tanabe et al., 2010; Takeuchi et al., 2015a), indicating that the Tg lines can be used to mark both differentiating and differentiated cells. Here we used fluorescence-activated cell sorting (FACS) to isolate granule cells, Purkinje cells, eurydendroid cells, IO neurons, and Bergmann glial cells from mid-larvae zebrafish of these Tg lines, and analyzed the transcriptomes in these cells.

Materials and Methods

Zebrafish lines

The Purkinje-cell-specific line aldoca:GAP-Venus (rk22Tg in ZFIN: http://zfin.org/) was described previously (Tanabe et al., 2010; Takeuchi et al., 2015a). In this line, membrane-tagged Venus is expressed under the control of the promoter of *aldolase Ca* (*aldoca*), which encodes zebrin II. The granule-cell-specific line gSA2AzGFF152B, the eurydendroid cell line hspzGFFgDMC156A, the IO-neuron line hspGFFDMC28C, and the Bergmann glia line SAGFF(LF)251A are gene/enhancer trap lines that express a modified version of Gal4-VP16 (GFF) (Asakawa et al., 2008), as previously reported (Takeuchi et al., 2015a). To visualize these cells, Gal4 Tg lines were crossed with UAS:GFP (nkuasgfp1aTg), and GFP-expressing cells were harvested from the resultant larvae. Wild-type zebrafish with the Oregon AB genetic background (RRID:ZIRC_ZL1) were used for *in situ* hybridization. The zebrafish were maintained in an environmentally controlled room at the Bioscience and Biotechnology Center, Nagoya University. The animal work in this study was approved by Nagoya University Animal Experiment Committee (approval number: 2014020503, 2015022304, 2016022203) and was conducted in accordance with “Regulations on Animal Experiments in Nagoya University” and “Guidelines for Proper Conduct of Animal Experiments (Science Council of Japan)”.

Immunohistochemistry

For immunostaining, anti-GFP (1:1000, rat, Nacalai Tesque, Cat# 04404-84 RRID:

AB_10013361) was used as described previously (Bae et al., 2009; Kani et al., 2010). Alexa Fluor 488 goat anti-rat IgG (H+L, Molecular Probes) was used as the secondary antibody. SeeDB reagent was prepared for the optical clearing of some fixed samples as described previously (Ke et al., 2013; Ke and Imai, 2014). Staining of the brains of the 14-dpf control larvae with the anti-GFP antibody gave no immunostaining signals (Fig. 1F). Fluorescence images were captured with an MZ16FA Leica fluorescence dissection microscope or an LSM700 confocal laser-scanning microscope (Zeiss). Images were constructed from Z-stack sections by the 3D projection program associated with the microscope (Zen, Zeiss). The figures were constructed using Adobe Photoshop and Adobe illustrator. Adjusting brightness and contrast of digital images was applied equally to all the images in each figure.

In situ hybridization

The *vglut1*, *aldoca*, and *cxcr4* were detected as described previously (Miyasaka et al., 2007; Bae et al., 2009). To make riboprobes for candidate genes, ~500-bp cDNA fragments were obtained by reverse-transcriptase (RT)-PCR from 5-dpf larvae using ReverTra Ace, KOD-Plus, Blend Taq (Toyobo), and GoTaq (Promega). The fragments were subcloned to pTAC-2 (BioDynamics Laboratory, Inc.) or pBluescript II SK+ (Agilent Technologies) after digestion with restriction enzymes. The primers used for RT-PCR are described in Table 1. To detect *tlx3b*, the cDNA fragment corresponding to nucleotides 596–1766 of NM_170766 (GenBank) was amplified by RT-PCR and subcloned to pGEM-T Easy (Promega). Riboprobes were generated from the linearized plasmids using digoxigenin-UTP (Roche) and T3, T7, or SP6 RNA Polymerase

(Promega).

We fixed 5-dpf larvae overnight at 4 °C in 4% paraformaldehyde (PFA) in phosphate-buffered saline (PBS). Whole-mount *in situ* hybridization of zebrafish larvae was performed as described previously (Thisse and Thisse, 1998), except that the hybridization was performed at 65 °C. For sectioning, the brain was removed from adult zebrafish, fixed overnight at 4 °C in 4% PFA/PBS, frozen in O.C.T. Compound (Sakura FineTechnical), and sectioned at 12–14 μm on a cryostat. *In situ* hybridization of the sections was carried out as described previously (Bae et al., 2009). To detect the signals from section and whole-mount *in situ* hybridization, BM Purple or NBT/BCIP (Roche) was used as a substrate for the alkaline phosphatase. Signals were acquired using an AxioPlan-2 microscope and an AxioCam CCD camera (Zeiss).

Cell dissociation

GFP/Venus-positive cells were isolated from the zebrafish Tg larvae using a protocol modified from a previous publication (Cerda et al., 2009). After anesthetizing 14-dpf larvae in cold Ringer's solution (123 mM NaCl, 1.5 mM $CaCl_2$, 5 mM KCl), the brain region was removed from the larvae with a 10-ml syringe and 27-gauge needle (Terumo). The hindbrain region including the cerebellum was dissected with a needle, and the samples were kept in 3% fetal bovine serum (FBS)/PBS (Life Technologies) on ice. The cells were dissociated using the Papain Dissociation System (Worthington Biochemical Corporation) according to the manufacturer's protocol. The hindbrain samples were incubated in 20 units/ml papain in Earle's Balanced Salt Solution (EBSS) and then pipetted up and down several times using a p-200 pipette. After a 1-h

incubation at 37 °C and repeated pipetting, the dissociated cells were harvested by centrifugation at 1,500 rpm, 430 x g, 4 °C for 5 min. The cell pellets were suspended in 0.5 ml of EBSS containing 100 units/ml DNase I, 1 mg/ml ovomucoid protease inhibitor, and 1 mg/ml bovine serum albumin (BSA). An albumin-inhibitor solution (10 mg/ml ovomucoid protease inhibitor and 10 mg/ml BSA) was added, and the cells were harvested by centrifugation at 1,500 rpm, 430 x g, 4 °C for 5 min. The cell pellets were resuspended in 3% FBS/PBS, and the completely dissociated cells were harvested by passing them through a cell strainer (35-μm pore size, BD Biosciences).

FACS and RNA isolation

Cell samples from 100–200 Tg larvae were sorted using a FACS Aria III Cell Sorter (BD Biosciences) according to the manufacturer's protocol. GFP/Venus signals were obtained using a 488-nm laser and the FITC filter set. Forward scatter (FSC) and side scatter (SSC) were used to evaluate the cell size and granularity, respectively, of cell populations. GFP- or Venus-positive cells were selected using four sequential gates (G1-4), as described in Fig.1: First, we removed (G1) dead cells, selected as a population with high SSC-A signals and confirmed by co-staining with propidium iodide; (G2) aggregated cells (a population containing more than one cell showing high FSC signals); and (G3) cells having high granularity (the non-neuronal, non-glial cell population). After selection with G1–G3, FITC signal-positive cells were selected (G4), as their signal strength was unambiguously higher than that of the FITC-negative major population. The sorted cells were collected directly into a tube containing 750 μl of TRIzol LS Reagent (Life Technologies), and 3% FBS/PBS was added for a total volume

of 1 ml. The samples were mixed by a vortex mixer and kept at −80 °C. After thawing the samples and adding 200 µl chloroform, the samples were again mixed with a vortex mixer. The aqueous phase containing RNA was recovered by centrifugation at 15,000 rpm, 20,400 x g, 4 °C, 15 min. Total RNA was isolated from the aqueous-phase solution using the RNeasy Mini Kit (Qiagen) according to the manufacturer's protocol. The amount of RNA was measured using an Agilent 2100 Bioanalyzer (Agilent Technologies) with the RNA 6000 Pico LabChip kit. More than one RNA sample was prepared for all cell types except the SAGFF(LF)251A (Bergmann glial) cells: for SAGFF(LF)251A; UAS:GFP cells, the GFP-expressing cells were collected once and divided into two tubes, and the RNA was prepared independently with TRIzol and the RNeasy Mini Kit. The number of larvae and harvested cells and the RNA quantities are described in Table 2.

Whole-transcriptome amplification

Whole-transcriptome amplification (WTA) using 1 ng total RNA was performed with the Quartz-Seq protocol (available at http://bit.accc.riken.jp/protocols/) (Sasagawa et al., 2013) modified to accommodate a cell mass instead of single cells, as follows. Reverse transcription was primed with 2.0 µl priming buffer using RNA dissolved in 1 µl RNase-free water as templates. The volume of the RT buffer was increased to 2.0 µl. After reverse transcription, the cDNA was purified using Agencourt AMPure XP (Beckman Coulter Inc.) to reduce the volume to 2.0 µl, and subjected to the standard Quartz-Seq protocol. Later, PCR for double-stranded cDNA amplification was performed with 15 cycles. The amplified DNA (10 ng) was diluted in 130 µl of

Tris-EDTA (TE) buffer and fragmented using a focused ultrasonicator (Covaris E220) with the following settings: duty factor, 10%; peak incident power, 175 W; cycles per burst, 100; and time, 600 seconds. The fragmented DNA was purified with DNA Clean and Concentrator-5 (Zymo Research) and eluted into 20 µl of nuclease-free water.

Library preparation for transcriptome analysis

DNA sequencing libraries were prepared based on the LIMprep protocol (the Quartz-Seq version, available at http://bit.accc.riken.jp/protocols/) (Sasagawa et al., 2013) modified as follows: 30 µl of the reaction mix containing 5.0 µl KAPA End Repair Buffer and 2.5 µl KAPA End Repair Enzyme Mix (Kapa Biosystems) was added to 20 µl of the fragmented DNA solution in end repair reactions. An adapter ligation mix containing 5 pmol of adapters equivalent to TruSeq adapters was prepared in-house.

Sequencing and quality control

The prepared libraries were sequenced to obtain paired-end reads using the Rapid Run mode on an Illumina HiSeq 1500 operated by HiSeq Control Software v2.0.12.0, using the Rapid SBS kit v1 with 100 cycles, and adding 5% PhiX spike-in to each lane. Base calling was processed with Real-Time Analysis (RTA) version 1.17.21.3 and converted to FASTQ-format files using bcl2fastq Conversion Software version 1.8.3 (Illumina Inc.). The FASTQ files were deposited in the DDBJ Sequence Read Archive (DRA) database (RRID: SCR_001370, accession number: PRJDB4941). Low-quality bases (quality value, $Q < 20$) , were removed from the 3′-end using the fastq_quality_trimmer in the FASTX Toolkit version 0.0.13

(http://hannonlab.cshl.edu/fastx_toolkit/index.html). Next, low-quality reads, defined as reads in which less than 80% of the bases had a Q≥20, were removed using the fastq_quality_filter in the FASTX Toolkit. The WTA and TruSeq adapters were trimmed using cutadapt version 1.2.1, setting the minimum overlap length between reads and the adapter at 1 bp (Martin, 2011) after removing reads shorter than 25 bp. Reads retained as pairs were used to analyze the gene expression and differential gene expression.

Analysis of gene expression levels and differential expression

The paired-end reads were mapped to the zebrafish genome assembly Zv9 using TopHat2 version 2.0.8b (Kim et al., 2013) assuming exon-intron boundaries based on the zebrafish genome annotation provided by Ensembl release 75 (Cunningham et al., 2015). Gene expression levels were quantified with Cuffdiff version 2.1.1 (Trapnell et al., 2010) using the zebrafish genome annotation, and a hierarchical clustering based on the gene expression profiles was performed with pvclust version 1.2.2 (Suzuki and Shimodaira, 2006). Differentially expressed genes were identified between two selected cell types using edgeR version 3.2.3 (Robinson et al., 2010), and p-values produced by the edgeR package were subjected to multiple corrections with the qvalue package version 1.34.0 (Storey, 2003). These computations were processed with default parameters of individual programs.

Gene ontology analysis

Gene Ontology (GO) enrichment analysis was performed with the web toolkit g:Profiler using the zebrafish gene set of Ensembl release 75

(http://biit.cs.ut.ee/gprofiler_archive/r1270_e75_eg22/web/) (Reimand et al., 2007; Reimand et al., 2011). Relationships between the products of differentially expressed genes identified in this study were investigated using the Kyoto Encyclopedia of Genes and Genomes (KEGG) pathway database (RRID: SCR_001120) (Ogata et al., 1999; Kanehisa and Goto, 2000). The hierarchical filtering of GO terms was performed with the “best per parent” method (g:profiler) to remove redundancies.

Results

Gene expression profiles of cerebellar cells

To understand the molecular mechanisms controlling the development and functions of the cerebellar circuits in zebrafish, we examined the gene expression profiles of cells involved in the neural circuitry of the cerebellum. We used five zebrafish Tg lines that express a fluorescent marker protein in specific types of cells (Fig. 1A-E). The aldoca:GAP-Venus line expresses membrane-tagged Venus specifically in Purkinje cells from the early larval stage (3 dpf) to adulthood (Tanabe et al., 2010; Takeuchi et al., 2015a). We used the Gal4 gene/enhancer trap lines gSA2AzGFF152B, hspzGFFgDMC156A, hspGFFDMC28C, and SAGFF(LF)251A crossed with the UAS:GFP reporter line to visualize cells (Asakawa et al., 2008; Takeuchi et al., 2015a) as follows. The gSA2AzGFF152B line expresses Gal4 specifically in granule cells in the anteromedial lobes (the valvula cerebelli and corpus cerebelli) of the cerebellum in larvae and adults (Takeuchi et al., 2015a). The hspzGFFgDMC156A, hspGFFDMC28C, and SAGFF(LF)251A lines express the reporter in eurydendroid cells, IO neurons, and

Bergmann glial cells, respectively, but also express Gal4 in other cells outside the cerebellum in larvae and adults (Takeuchi et al., 2015a). All of the Tg lines can label cells beginning in the early larval stage (3 dpf) (Takeuchi et al., 2015a). In zebrafish, granule cells and Purkinje cells are continuously generated from their progenitors during the larval stage (2–30 dpf) (Kani et al., 2010). We hypothesized that the cerebellum from the mid-larval stage (12-20 dpf) should contain both differentiating and differentiated neurons and glial cells. We confirmed the expression of the Venus or GFP fluorescent marker in the cerebellar neurons or the IO neurons at 14 dpf (Fig. 1A-E). We dissected out the brain from about 100–200 14-dpf larvae from each Tg line and isolated the hindbrain region containing the cerebellum and the IOs. After dissociating the cells with papain, we collected Venus/GFP-expressing cells by FACS and extracted their total RNA for RNA-seq (Fig. 1G, H, I, and Table 2). Since the amount of RNA was insufficient for standard RNA-seq library preparation, we used the Quartz-Seq protocol, a combination of unbiased PCR-mediated amplification and RNA-seq that was originally introduced for single-cell transcriptome analyses (Sasagawa et al., 2013). We performed Quartz-seq WTA using 1 ng of total RNA, preparing two or three library replicates for each cell type, and the prepared libraries were sequenced to obtain 9.2–10.7 million reads per library (Table 2). The obtained reads were trimmed and mapped to the zebrafish reference genome to quantify expression levels of individual genes (Suppl. Table 1).

Validation of the transcriptomes of Purkinje cells and granule cells

To validate our strategy for the transcriptome analysis, we first compared the expression of various marker genes (Table 3). The *vglut1* (*slc17a7*), *neurod*, and *reelin* (*reln*) genes are well known markers for granule cells in the zebrafish cerebellum (Costagli et al., 2002; Bae et al., 2009). Although the expression level of *vglut1* was relatively low, it was specific to the granule-cell Tg line gSA2AzGFF152B. The expression of *neurod* and *reelin* was much higher in the GFP^+ cells in gSA2AzGFF152B larvae (152B; UAS:GFP^+) than in those of larvae of other lines (Table 3). We found that *aldoca*, parvalbumin7, and carbonic anhydrase 8 (*ca8*), which are specific markers for Purkinje cells, and *lhx1a* and *gad1b*, which are expressed in Purkinje cells in the zebrafish cerebellum (Bae et al., 2009), were expressed at much higher levels in the $Venus^+$ cells in aldoca:GAP-Venus larvae than in GFP^+ cells in the other Tg lines (Table 3, aldoca columns). We also showed that the 152B; UAS:GFP^+ and aldoca:GAP-$Venus^+$ cells, respectively, expressed other granule-cell-specific and Purkinje-cell-specific genes, including genes that are known to be expressed by mammalian granule cells and Purkinje cells (Table 6, 7; see below). These data indicate that 152B; UAS:GFP^+ and aldoca:GAP-$Venus^+$ cells, respectively, represent granule cells and Purkinje cells in the zebrafish larval cerebellum.

We previously reported that eurydendroid cells express *vglut2a* (*slc17a6b*), and that a portion of eurydendroid cells express the proneural gene *olig2* (Bae et al., 2009; Kani et al., 2010). In the present study, we found that *olig2* and *vglut2a* were expressed at much higher levels in GFP^+ cells in the hspzGFFgDMC156A; UAS:GFP larvae than in those of the other lines (156A, Table 3). The IO neurons are located in the posterior hindbrain, and express *hoxb5a* and other *hox* genes that are expressed in the

posterior hindbrain. We previously reported that IO neurons express *vglut2a* and *pou4f1* (Bae et al., 2009). In the present study, our RNA-seq data indicated that *hoxb5a*, *vglut2a*, and *pou4f1* were expressed in the GFP^+ cells in the hspGFFDMC28C; UAS:GFP larval hindbrain at higher levels than in those of the other lines (28C, Table 3). We detected that *fabp7a*, a marker of Bergmann glial cells, was strongly expressed in GFP^+ cells in the SAGFF(LF)251A larval hindbrain, but was also expressed in other cell types (251A, Table 3). However, we found that GFP^+ cells from the 156A, 28C, and 251A lines expressed unexpected genes; we used *in situ* hybridization to pick up several genes expressed at high levels, defined as FPKM (fragments per kilobase of exon per million mapped fragments) > 50, in GFP^+ cells in these lines and to examine their expression. We found that our results included contaminants in addition to the expected cell-type-specific genes. In particular, 28C; UAS:GFP^+ cells expressed many epithelial genes, including collagens, laminin, and keratins, suggesting that the population was contaminated with epithelial cells. This finding is consistent with previous data showing that GFP was detected in cells other than eurydendroid cells, IO neurons, and Bergmann glial cells in the 156A, 28C, and 251A lines (Takeuchi et al., 2015a). Clustering analysis revealed that the transcriptomes from the two samples of 152B; UAS:GFP^+ cells (granule cells) were related to each other, that those from the three aldoca:GAP-$Venus^+$ cell samples (Purkinje cells) were related to one another, and those from the 152B; UAS:GFP^+ cell samples were distantly related to the transcriptomes from aldoca:GAP-$Venus^+$ cell samples (28C data were excluded, Fig. 1J). In this report, we focused on transcriptomes in granule cells and Purkinje cells using the data from

152B; UAS:GFP$^+$ cells and aldoca:GAP-Venus$^+$ cells. We also examined a few genes from the list of genes expressed in 251A (glia) lines.

Comparison of the transcriptomes in granule cells and Purkinje cells

Differential expressions based on our RNA-seq data from granule cells and Purkinje cells were statistically assessed with among-replicate variations taken into account. We selected genes that were expressed at significantly higher levels in 152B; UAS:GFP$^+$ granule cells than in aldoca:GAP-Venus$^+$ cells, and vice versa. Of these, 1,077 genes were significantly upregulated in granule cells (hereafter referred as to "granule-cell genes"), and 887 genes were significantly upregulated in Purkinje cells ("Purkinje-cell genes") (Q-value < 0.01, Suppl. Table 2, 3). We analyzed the enrichment of these genes by GO and KEGG to determine which types of genes were more relevant to granule or Purkinje cells in the cerebellum of the larval zebrafish (Table 4, 5) (Reimand et al., 2007; Reimand et al., 2011). The GO classifies gene functions along three categories: Biological Processes (pathways and large processes made up to the activities of multiple gene products), Cellular Components (where gene products are active), and Molecular Function (molecular activities of gene products) (http://geneontology.org) (Ashburner et al., 2000). In the Biological Processes category, the granule-cell genes were enriched in genes involved in the development of neurons, including transcription factors and signaling molecules. In the Cellular Component category, the granule-cell genes were enriched in genes related to synapses and synaptic vesicles, whereas the Purkinje-cell genes were enriched in genes for transmembrane transporters, such as ion transporters. Similarly, in the Molecular Function category, the Purkinje-cell genes were enriched in

transmembrane transporter genes. KEGG pathway analysis (Ogata et al., 1999; Kanehisa and Goto, 2000) indicated that the granule-cell genes were enriched in genes related to cell signaling such as the MAP kinase (MAPK) and Notch signaling pathways involved in neuron proliferation and differentiation, while the Purkinje-cell genes were enriched in genes involved in the Ca^{2+} signaling pathway (Table 4, 5).

Expression of granule-cell and Purkinje-cell genes in the early larval and adult brain

To verify and analyze the expression of granule-cell and Purkinje-cell genes, we selected major granule-cell genes with relatively high expression (FPKM value > 40) that were expressed in 152B; UAS:GFP^+ cells at levels at least 10 times higher than in aldoca:GAP-$Venus^+$ cells (Table 6). We selected major Purkinje-cell genes in the same way (Table 7). In addition to these criteria, we also picked up genes that were expressed at high levels but had a relatively low fold difference in expression (152B/aldoca or aldoca/152B), and considered their possible biological significance for further analysis. We examined the expression of high-ranking genes (genes with a high FPKM) by *in situ* hybridization with 5-dpf larvae (in which granule cells and Purkinje cells are just beginning to differentiate) and in the adult brain (Fig. 2–11). Most of the high-ranking granule-cell- and Purkinje-cell-specific genes (FPKM > 80 in 152B; UAS:GFP, and FPKM > 100 in aldoca:GAP-Venus) were expressed at detectable levels in granule cells and Purkinje cells, respectively, at 5 dpf (Fig. 2-4, 6-10). Our data indicated that many granule-cell and Purkinje-cell genes expressed at the mid-larval stage are also expressed as these cells begin to differentiate. Although the major granule-cell and Purkinje-cell

genes include genes that are expressed in the cerebellum of other vertebrate species, they also include genes whose cerebellar expression has not been reported. We will further discuss differences in granule-cell and Purkinje-cell transcriptomes between zebrafish and other vertebrates in the Discussion.

We found that many granule-cell genes were expressed at levels that were too low to detect by the *in situ* hybridization of sections prepared from the adult cerebellum. Nevertheless, we found that the granule-cell genes *neurod*, *cbln12*, *fat2*, and *wu:fj39g12* were expressed by granule cells in the adult cerebellum as well as those in the torus longitudinalis, which is part of a cerebellum-like structure (Fig. 5). We found that more Purkinje-cell than granule-cell genes were expressed in the adult cerebellum (Fig. 11). Of these, *aldoca*, *hpca*, *C15H11orf87*, *rgs3a*, *ca8*, *grm1a*, *lingo4b*, and *itpr1b* were expressed only in Purkinje cells (Fig. 11B-I), whereas *pvalb7* and *grid2ipa* were expressed not only in Purkinje cells, but also in neurons in the optic tectum and the MON (Fig. 11A, J), probably corresponding to type I neurons and crest cells, respectively (Bae et al., 2009; Hibi and Shimizu, 2012). Our findings revealed that *neurod*, *cbln12*, *fat2*, and *wu:fg39g12* expressed in granule cells and *grid2ipa* expressed in Purkinje cells/type I neurons/crest cells are additional members of the gene set shared among the cerebellum-like structures.

Bergmann glial genes

Transcriptome data from the SAGFF(LF)251A; UAS:GFP line contained genes that were not Bergmann glial genes. However, by comparing transcriptomes in 251A cells with those of other cell types, and by *in situ* hybridization, we were able to pick up a

few genes specifically expressed in Bergmann glial cells. We found that *grik2* (glutamate receptor, inotropic, kainate 2, CR933820.2) was expressed in Bergmann glial cells in the larval cerebellum and in the molecular layer of the adult cerebellum, but not in ependymal cells (Fig. 12), and that *gdf10a* and *gdf10b* were expressed in larval Bergmann glial cells (Fig. 12A).

DISCUSSION

Zebrafish transcriptome analysis using Tg lines

In this report, we analyzed transcriptomes in zebrafish gene/enhancer trap lines and in Tg lines that expressed a fluorescent protein under the control of the cell-type-specific promoter *aldoca*. The transcriptomes from the gSA2AzGFF152B; UAS:GFP and aldoca:GAP-Venus lines represented the expression profiles of granule cells and Purkinje cells, respectively. Previous reports also show that these Tg lines specifically express GFP/Venus in granule cells and Purkinje cells (Tanabe et al., 2010; Takeuchi et al., 2015a). RNA profiles (microarray or RNA-seq) have been reported for FACS-sorted cells from zebrafish Tg lines (Cerda et al., 2009; Stuckenholz et al., 2009; Qin and Raymond, 2012; Gallardo and Behra, 2013; Jiang et al., 2014; Ristori and Nicoli, 2015), and many Tg lines, including Gal4 trap lines, are available for marking different types of neurons in zebrafish (Asakawa et al., 2008). Thus, zebrafish Tg lines, FACS, and RNA profiling can be combined to further investigate the molecular nature of the individual types of neurons that compose the neural networks in zebrafish. However, it should be noted that the transcriptomes from some Gal4 lines are known to contain

contamination from other cell types (e.g., epithelial cells for hspGFFDMC28C). Many of the trap lines express reporter genes in cells other than the neurons of interest due to the nature of the trapped genes or from amplification via the Gal4-UAS and heat-shock promoter systems. Establishing more cell-type-specific Tg lines or finding methods to filter out non-specific genes may be necessary for the precise analysis of transcriptomes in some types of neurons and glial cells. Although transcriptomes from the eurydendroid-cell Tg line hspzGFFgDMC156A and the IO-neuron Tg line hspzGFFDMC28C include contaminants, they should also include genes that are expressed by eurydendroid cells or IO neurons. As the nature of these neurons, particularly eurydendroid cells, is not well understood, further transcriptome analysis is needed to characterize them. In addition, the cerebellum of teleosts includes Golgi and stellate cells (Butler and Hodos, 1996; Meek et al., 2008; Bae et al., 2009), which we did not analyze in this study. Future transcriptome analysis with Tg lines expressing a fluorescent protein in Golgi and/or stellate cells should facilitate our understanding of the molecular nature of these GABAergic cerebellar interneurons.

Comparison of transcriptomes in granule cells and Purkinje cells

We compared the transcriptomes in granule cells and Purkinje cells from zebrafish in the mid-larval stage, and found that developmental genes were significantly expressed in granule cells (Table 4, 5). Many proneuronal genes, such as the *neurod*-family genes that regulate neuronal differentiation, were upregulated in granule cells but not in Purkinje cells in mid-larval zebrafish (Table 6, Fig 2-4). Enrichment analysis revealed that the granule-cell genes were also enriched in genes involved in the MAPK signaling

pathway, including *fgf8a*, *fgf13b*, *fgfr4*, *map2k1*, *map2k2a*, *mapk10*, *mapk11*, *dusp5*, and *dusp7* (KEGG:04010, Table 4, 6, Suppl. Table 2). Among these, we found that *fgf8a*, *mapk11*, and *dusp5* were expressed beginning at 5 dpf (Fig. 3). Fgf ligands (e.g., Fgf8a and Fgf13b) activate the MAPK signaling pathways (MAP2K1 and MAP2k2a are MAPK kinases; MAPK10 and MAPK11 are MAPKs), and Dusps (MAPK phosphatases) function as feedback regulators (*dusp* expression is correlated with the strength of MAPK signaling). Given that Fgf-MAPK signaling is involved in the growth of the cerebellum in larvae and adult fish (Kaslin et al., 2009), our data suggest that granule-cell progenitors and immature granule cells receive continuous growth signals from the early larval stage. In addition, as *fgf12a* was expressed in Purkinje cells (Table 7), Fgf12a from Purkinje cells may contribute to activating the MAPK signaling pathway in granule cells. Many cell-cycle regulators were upregulated in granule cells, including *ccnb1*, *ccnb3* (Cyclin B), *ccng2* (Cyclin G2), and *cdkn1ba* (p27) (Suppl. Table 2). These upregulations are correlated with the continuous proliferation of granule cells at the mid-larval stage (Zupanc et al., 2005; Kaslin et al., 2009; Kani et al., 2010; Kaslin et al., 2013). In contrast, genes involved in intercellular signaling were expressed at significant levels in Purkinje cells. Larval Purkinje cells retained a high expression of Ca^{2+}-related genes, transporters/channels, and metabolic enzymes (Table 5, 7). Ca signaling is important for integrating signals from the climbing fibers and parallel fibers, and in the synaptic plasticity of Purkinje cells (Kitamura and Kano, 2013; Mikoshiba, 2015). Our data suggest that the majority of larval Purkinje cells are differentiated and already functioning to integrate the signals from the IO and granule cells. Our RNA-seq data were consistent with the observation that Purkinje cells terminate neurogenesis

earlier than granule cells and start performing neuronal functions (Kaslin et al., 2013). Our gene expression profiling, enabled by a suitable protocol for the targets of this study, indicated that granule cells are still in the process of neural differentiation at the mid-larval stage, whereas a major population of Purkinje cells are already terminally differentiated and have begun to express neuronal-function genes.

We noticed that the granule-cell genes show variation in their expression domains: some are expressed in all the granule cells (e.g. *cbln12*) but others are expressed in more specific domains (e.g. *fgf8a* anteriorly and *tlx3a* more posteriorly in the anteromedial lobes) (Fig. 2-4). In contrast, most of the Purkinje cell-genes are expressed to a greater or lesser extend in the same Purkinje cell population (Fig. 6-10). The differential expression of the granule-cell genes may correlate with functional differences of distinct granule cell populations. The corpus cerebelli of the teleost cerebellum is reported to be involved in classical conditioning or spatial cognition (Gomez et al., 2010; Yoshida and Hirano, 2010; Duran et al., 2014), whereas the caudolateral lobes of the teleost cerebellum are connected to the octavolateral system (MON/DON) (Bae et al., 2009; Volkmann et al., 2010; Wullimann and Grothe, 2014; Takeuchi et al., 2015b) and may be involved in motor learning and/or regulation of body balance. Granule cells in the corpus cerebelli and the caudolateral lobes should have distinct functions. The differentially expressed granule-cell genes may be involved in function and/or development of the distinct granule cell populations. Alternatively, some granule-cell genes, such as *fgf8a*, may be involved in growth and/or differentiation of specific types of cells in the cerebellum or adjacent brain regions (e.g. tegmentum).

Differences in granule-cell and Purkinje-cell genes in mammals and zebrafish

We found many granule cell- and Purkinje cell-specific genes that are shared by zebrafish and mammals. We also identified genes whose functions are not well studied in mammalian cerebella (Fig. 2–11). For example, orthologues of the transcriptional regulator genes *neurod*, *nfia*, *tlx3a/b*, and *pax6a* are expressed in granule cells in mammals, and gene-knockout studies in mice show that *Neurod*, *NfI*, and *Pax6* are important for the differentiation, cell polarization, and migration of granule cells (Engelkamp et al., 1999; Miyata et al., 1999; Yamasaki et al., 2001; Lopes et al., 2006; Schuller et al., 2006; Wang et al., 2007; Wang et al., 2010). These genes likely play similar roles in zebrafish granule cells. In contrast, the expression of *prdm8b* and *uncx4.1* orthologues in mammalian granule cells has not been reported. Mouse *Prdm8* is expressed in the upper layer of the neocortex, and a *Prdm8* deficiency reduces the number of upper-layer neocortical neurons (Inoue et al., 2015). *Uncx4.1* expressed in the hypothalamic magnocellular neurons is involved in the establishment of hypothalamic projection to the neurohypophysis in mice (Asbreuk et al., 2006). *Uncx4.1* is also involved in the differentiation of midbrain dopaminergic neurons (Rabe et al., 2012). Although the functions of *Prdm8* and *Uncx4.1* in mammalian granule cells have not been described, they may be involved in the differentiation and/or axon pathfinding of zebrafish granule cells.

Orthologues of the transcriptional regulator genes *skor2* (*Corl2)* and *foxp4* are expressed in mammalian Purkinje cells; *Skor2* and *Foxp4* are involved in the maturation of Purkinje cells and the maintenance of Purkinje-cell dendrites, respectively (Minaki et

al., 2008; Tam et al., 2011; Nakatani et al., 2014), suggesting that these genes have similar roles in zebrafish Purkinje cells. In contrast, the expression of *skor1b*, *foxp1b*, and *rorb* orthologues, or of the putative transcriptional regulator genes *znf385c* and *pbxip1b*, has not been reported in mammalian Purkinje cells, and it remains to be determined whether these genes are involved in Purkinje-cell development in mammals or if they have zebrafish (or teleost)-specific roles. As the expression of these granule-cell- and Purkinje-cell-specific transcriptional regulator genes was detected beginning at 5 dpf (Fig. 2-4, 6-10), these transcriptional regulators may contribute to the differentiation and maturation of granule cells and Purkinje cells. As reported for mammals, the granule cells and Purkinje cells in zebrafish are distinct cell lineages derived from distinct neuronal progenitors located in the upper rhombic lip and ventricular zone, respectively (Kani et al., 2010). The differential expression of transcriptional regulators between granule and Purkinje cells should reflect that these two cell types employ distinct genetic programs for their neuronal differentiation and maturation. Generating zebrafish mutants of these genes and analyzing their phenotypes should reveal their roles in the development of granule cells and Purkinje cells, and may further identify hierarchal cascades of transcriptional regulators involved in granule-cell and Purkinje-cell development.

The signaling molecules involved in forming the layers and neural circuits of the cerebellum are conserved between zebrafish and mammals. Reelin is important for the migration of Purkinje cells and the formation of the Purkinje-cell layer (Mariani et al., 1977; D'Arcangelo et al., 1995). In mice, Reelin protein secreted from immature granule cells is received as a signal by Purkinje cells (Miyata et al., 2010). Similarly,

reelin is expressed in granule cells, and *dab1a* and *vldlr*, which encode molecules involved in Reelin signaling, are expressed in Purkinje cells in zebrafish (Costagli et al., 2002; Imai et al., 2012) (Fig. 3, Suppl. Table 2, 3). Cbln1 (cerebellin1) secreted from granule cells and Grid2 (glutamate receptor, ionotropic, delta 2) on Purkinje-cell dendrites play a pivotal role in forming synapses between granule cells and Purkinje cells (Matsuda et al., 2010; Uemura et al., 2010). In zebrafish, *cbln12*, a putative orthologue of mouse *Cbln1* (zebrafish *cbln1* and *cbln12* are probably paralogous) is specifically expressed in granule cells, and *grid2* is expressed in Purkinje cells (Mikami et al., 2004) (Fig. 3, Suppl. Table 2, 3). We also found that zebrafish Purkinje cells expressed *grid2ipa*, a gene that encodes the Grid2-interacting protein A (also known as Delphilin) (Fig. 8), which modulates synaptic transmission between granule cells and Purkinje cells (Takeuchi et al., 2008). Sema7a is involved in eliminating synapses between climbing fibers and Purkinje cells at postnatal stages in mice (Uesaka et al., 2014). Although it is not known whether this elimination of climbing-fiber synapses also occurs in zebrafish, it is intriguing to speculate that a remodeling process takes place at the early larval stages. However, Sema7a may have a different role in the formation of cerebellar neural circuits in zebrafish. In any case, our data suggest that the same or similar molecular mechanisms form and remodel the cerebellar neural circuits in zebrafish and mammals.

The cerebellum and cerebellum-like structures

The cerebellum-like structures, which have a neural circuit structure similar to the cerebellum, include the MON/DON and the marginal layer of the optic tectum in

zebrafish (Bell, 2002; Bell et al., 2008; Hibi and Shimizu, 2012). Like the Purkinje cells in the cerebellum, type I neurons in the optic tectum and crest cells in the MON/DON receive inputs from granule cells in the torus longitudinalis and the caudolateral lobes (the eminentia granularis and lobus caudalis cerebelli) of the cerebellum, respectively. Several genes are shared among the cerebellum-like structures (Mikami et al., 2004; Katsuyama et al., 2007; Bae et al., 2009). In this report, we found that the expression of *cbln12* and *fat2* (FAT atypical cadherin 2) was shared by granule cells in the torus longitudinalis and the cerebellum, and that *grid2ipa* expression was shared by Purkinje cells, type I neurons, and crest cells (Fig. 5, 11). Considering the role of the Cbln–Grid2 system in synapse formation (Matsuda et al., 2010; Uemura et al., 2010) and the Fat2 protein's specific localization on the parallel fibers of mammalian granule cells (Nakayama et al., 2002), the neural-circuit formation of the cerebellum-like structures is controlled at least in part by common molecular mechanisms.

Bergmann glia

Bergmann glial cells, which are a type of astrocyte in the cerebellum, modulate the activity of cerebellar neural circuits. Grik2 (glutamate receptor, ionotropic kinase 2) is expressed specifically in the Bergmann glia in the chick cerebellum (Gregor et al., 1989). We found that *grik2* was also expressed in Bergmann glial cells in zebrafish (Fig. 12). Grik2 may be involved in the Bergmann glial cell–mediated modulation of the neuronal connectivity that is conserved among vertebrates. In mice, the expression of *Gdf10*, one of the *Bmp*-family genes, is detected in both the rhombic lip and ventricular zone at prenatal stages but is restricted to Bergmann glial cells at the postnatal stages

(Mecklenburg et al., 2014). We observed a similar expression profile for *gdf10a/b* in zebrafish (Fig. 12). Although a Gdf10 deficiency does not lead to apparent defects in cerebellar development in mice (Zhao et al., 1999), Gdf10 is involved in the axon outgrowth (recovery) of cortical neurons in mice after a stroke (Li et al., 2015). As *gdf10a/b* is expressed in the molecular layer, where granule-cell axons grow, Gdf10a/b may support the remodeling of granule-cell axons in a feature that is relatively specific to the zebrafish cerebellum.

Although the microcircuit structure of the cerebellum is fairly conserved among vertebrates, there is wide variation in the gross morphology, and possibly the functions, of the cerebellum (Butler and Hodos, 1996; Altman and Bayer, 1997). Comparing cerebellar transcripts in zebrafish (in this study), mice (Schuller et al., 2006; Sato et al., 2008; Furuichi et al., 2011; Ha et al., 2015), and other vertebrate species should lead to a better understanding of common developmental mechanisms and functions of the cerebellum, as well as the mechanisms underlying species-specific features of cerebellar neural circuitry.

ACKNOWLEDGMENTS

We thank K. Kawakami for the Gal4 trap lines, Y. Sonobe for technical assistance with the FACS, K. Ihara for technical assistance with the RNA quantification, T. Hayashi and O. Nishimura for technical assistance with the RNA-seq, K. Kondoh and S. Tsukazaki

for fish care, the National Bioresource Project (NBRP) for zebrafish maintenance and providing the Tg lines, and the members of the Hibi Laboratory for helpful discussions.

CONFLICT OF INTEREST STATEMENT

The authors declare no conflicts of interest.

ROLE OF AUTHORS

All authors had full access to all of the study data and take responsibility for the integrity of the data and accuracy of the data analysis. MH conceived and designed the study. MT, SY, MS, TH, KM, YH, and CT acquired the data. MT, SY, MS, KM, YH, TS, SK, and MH analyzed and interpreted the data. MH drafted the manuscript, and YH, TS, and SK provided critical revisions of the manuscript involving important intellectual content. TS and MH obtained funding for the study. MH supervised the study.

Literature Cited

Altman J, Bayer SA. 1997. Developmentof the cerebellar system in relation to its evolution, structure, and function: CRC Press, Inc., Boca Raton, FL.

Asakawa K, Suster ML, Mizusawa K, Nagayoshi S, Kotani T, Urasaki A, Kishimoto Y, Hibi M, Kawakami K. 2008. Genetic dissection of neural circuits by Tol2 transposon-mediated Gal4 gene and enhancer trapping in zebrafish. Proc Natl Acad Sci U S A 105:1255-1260.

Asbreuk CH, van Doorninck JH, Mansouri A, Smidt MP, Burbach JP. 2006. Neurohypophysial dysmorphogenesis in mice lacking the homeobox gene Uncx4.1. Journal of molecular endocrinology 36:65-71.

Ashburner M, Ball CA, Blake JA, Botstein D, Butler H, Cherry JM, Davis AP, Dolinski K, Dwight SS, Eppig JT, Harris MA, Hill DP, Issel-Tarver L, Kasarskis A, Lewis S, Matese JC, Richardson JE, Ringwald M, Rubin GM, Sherlock G. 2000. Gene ontology: tool for the unification of biology. The Gene Ontology Consortium. Nat Genet 25:25-29.

Bae YK, Kani S, Shimizu T, Tanabe K, Nojima H, Kimura Y, Higashijima S, Hibi M. 2009. Anatomy of zebrafish cerebellum and screen for mutations affecting its development. Dev Biol 330:406-426.

Bell CC. 2002. Evolution of cerebellum-like structures. Brain Behav Evol 59:312-326.

Bell CC, Han V, Sawtell NB. 2008. Cerebellum-like structures and their implications for cerebellar function. Annu Rev Neurosci 31:1-24.

Butler AB, Hodos H. 1996. Comparative Vertebrate Neuroanatomy: Evolution and Adaptation: Wiley-Liss, New York.

Cerda GA, Hargrave M, Lewis KE. 2009. RNA profiling of FAC-sorted neurons from the developing zebrafish spinal cord. Dev Dyn 238:150-161.

Costagli A, Kapsimali M, Wilson SW, Mione M. 2002. Conserved and divergent patterns of Reelin expression in the zebrafish central nervous system. J Comp Neurol 450:73-93.

Cunningham F, Amode MR, Barrell D, Beal K, Billis K, Brent S, Carvalho-Silva D, Clapham P, Coates G, Fitzgerald S, Gil L, Giron CG, Gordon L, Hourlier T, Hunt SE, Janacek SH, Johnson N, Juettemann T, Kahari AK, Keenan S, Martin FJ, Maurel T, McLaren W, Murphy DN, Nag R, Overduin B, Parker A, Patricio M, Perry E, Pignatelli M, Riat HS, Sheppard D, Taylor K, Thormann A, Vullo A,

Wilder SP, Zadissa A, Aken BL, Birney E, Harrow J, Kinsella R, Muffato M, Ruffier M, Searle SM, Spudich G, Trevanion SJ, Yates A, Zerbino DR, Flicek P. 2015. Ensembl 2015. Nucleic acids research 43:D662-669.

D'Arcangelo G, Miao GG, Chen SC, Soares HD, Morgan JI, Curran T. 1995. A protein related to extracellular matrix proteins deleted in the mouse mutant reeler. Nature 374:719-723.

Duran E, Ocana FM, Martin-Monzon I, Rodriguez F, Salas C. 2014. Cerebellum and spatial cognition in goldfish. Behavioural brain research 259:1-8.

Engelkamp D, Rashbass P, Seawright A, van Heyningen V. 1999. Role of Pax6 in development of the cerebellar system. Development 126:3585-3596.

Finger TE. 1978. Efferent neurons of the teleost cerebellum. Brain Res 153:608-614.

Furuichi T, Shiraishi-Yamaguchi Y, Sato A, Sadakata T, Huang J, Shinoda Y, Hayashi K, Mishima Y, Tomomura M, Nishibe H, Yoshikawa F. 2011. Systematizing and cloning of genes involved in the cerebellar cortex circuit development. Neurochemical research 36:1241-1252.

Gallardo VE, Behra M. 2013. Fluorescent activated cell sorting (FACS) combined with gene expression microarrays for transcription enrichment profiling of zebrafish lateral line cells. Methods 62:226-231.

Gomez A, Duran E, Salas C, Rodriguez F. 2010. Cerebellum lesion impairs eyeblink-like classical conditioning in goldfish. Neuroscience 166:49-60.

Gregor P, Mano I, Maoz I, McKeown M, Teichberg VI. 1989. Molecular structure of the chick cerebellar kainate-binding subunit of a putative glutamate receptor. Nature 342:689-692.

Ha T, Swanson D, Larouche M, Glenn R, Weeden D, Zhang P, Hamre K, Langston M, Phillips C, Song M, Ouyang Z, Chesler E, Duvvurru S, Yordanova R, Cui Y, Campbell K, Ricker G, Phillips C, Homayouni R, Goldowitz D. 2015. CbGRiTS: cerebellar gene regulation in time and space. Dev Biol 397:18-30.

Hashimoto M, Hibi M. 2012. Development and evolution of cerebellar neural circuits. Dev Growth Differ 54:373-389.

Hibi M, Shimizu T. 2012. Development of the cerebellum and cerebellar neural circuits. Developmental neurobiology 72:282-301.

Hoshino M. 2006. Molecular machinery governing GABAergic neuron specification in the cerebellum. Cerebellum 5:193-198.

Ikenaga T, Yoshida M, Uematsu K. 2005. Morphology and immunohistochemistry of efferent neurons of the goldfish corpus cerebelli. J Comp Neurol 487:300-311.

Ikenaga T, Yoshida M, Uematsu K. 2006. Cerebellar efferent neurons in teleost fish. Cerebellum 5:268-274.

Imai H, Oomiya Y, Kikkawa S, Shoji W, Hibi M, Terashima T, Katsuyama Y. 2012. Dynamic changes in the gene expression of zebrafish Reelin receptors during embryogenesis and hatching period. Dev Growth Differ 54:253-263.

Inoue M, Iwai R, Yamanishi E, Yamagata K, Komabayashi-Suzuki M, Honda A, Komai T, Miyachi H, Kitano S, Watanabe C, Teshima W, Mizutani K. 2015. Deletion of Prdm8 impairs development of upper-layer neocortical neurons. Genes to cells : devoted to molecular & cellular mechanisms 20:758-770.

Ito M. 2005. Bases and implications of learning in the cerebellum--adaptive control and internal model mechanism. Prog Brain Res 148:95-109.

Ito M. 2006. Cerebellar circuitry as a neuronal machine. Prog Neurobiol 78:272-303.

Ito M. 2008. Control of mental activities by internal models in the cerebellum. Nat Rev Neurosci 9:304-313.

Jiang L, Romero-Carvajal A, Haug JS, Seidel CW, Piotrowski T. 2014. Gene-expression analysis of hair cell regeneration in the zebrafish lateral line. Proc Natl Acad Sci U S A 111:E1383-1392.

Kanehisa M, Goto S. 2000. KEGG: kyoto encyclopedia of genes and genomes. Nucleic acids research 28:27-30.

Kani S, Bae YK, Shimizu T, Tanabe K, Satou C, Parsons MJ, Scott E, Higashijima S, Hibi M. 2010. Proneural gene-linked neurogenesis in zebrafish cerebellum. Dev Biol 343:1-17.

Kaslin J, Ganz J, Geffarth M, Grandel H, Hans S, Brand M. 2009. Stem cells in the adult zebrafish cerebellum: initiation and maintenance of a novel stem cell niche. J Neurosci 29:6142-6153.

Kaslin J, Kroehne V, Benato F, Argenton F, Brand M. 2013. Development and specification of cerebellar stem and progenitor cells in zebrafish: from embryo to adult. Neural Dev 8:9.

Katsuyama Y, Oomiya Y, Dekimoto H, Motooka E, Takano A, Kikkawa S, Hibi M, Terashima T. 2007. Expression of zebrafish ROR alpha gene in cerebellar-like structures. Dev Dyn 236:2694-2701.

Ke MT, Fujimoto S, Imai T. 2013. SeeDB: a simple and morphology-preserving optical clearing agent for neuronal circuit reconstruction. Nat Neurosci 16:1154-1161.

Ke MT, Imai T. 2014. Optical Clearing of Fixed Brain Samples Using SeeDB. Current protocols in neuroscience / editorial board, Jacqueline N Crawley [et al] 66:2

22 21-22 22 19.

Kim D, Pertea G, Trapnell C, Pimentel H, Kelley R, Salzberg SL. 2013. TopHat2: accurate alignment of transcriptomes in the presence of insertions, deletions and gene fusions. Genome Biology 14:R36.

Kitamura K, Kano M. 2013. Dendritic calcium signaling in cerebellar Purkinje cell. Neural networks : the official journal of the International Neural Network Society 47:11-17.

Li S, Nie EH, Yin Y, Benowitz LI, Tung S, Vinters HV, Bahjat FR, Stenzel-Poore MP, Kawaguchi R, Coppola G, Carmichael ST. 2015. GDF10 is a signal for axonal sprouting and functional recovery after stroke. Nat Neurosci 18:1737-1745.

Lopes C, Delezoide AL, Delabar JM, Rachidi M. 2006. BARHL1 homeogene, the human ortholog of the mouse Barhl1 involved in cerebellum development, shows regional and cellular specificities in restricted domains of developing human central nervous system. Biochem Biophys Res Commun 339:296-304.

Mariani J, Crepel F, Mikoshiba K, Changeux JP, Sotelo C. 1977. Anatomical, physiological and biochemical studies of the cerebellum from Reeler mutant mouse. Philos Trans R Soc Lond B Biol Sci 281:1-28.

Martin M. 2011. Cutadapt removes adapter sequences from high-throughput sequencing reads. EMBnetjournal 17:10-12.

Matsuda K, Miura E, Miyazaki T, Kakegawa W, Emi K, Narumi S, Fukazawa Y, Ito-Ishida A, Kondo T, Shigemoto R, Watanabe M, Yuzaki M. 2010. Cbln1 is a ligand for an orphan glutamate receptor delta2, a bidirectional synapse organizer. Science 328:363-368.

Mecklenburg N, Martinez-Lopez JE, Moreno-Bravo JA, Perez-Balaguer A, Puelles E, Martinez S. 2014. Growth and differentiation factor 10 (Gdf10) is involved in Bergmann glial cell development under Shh regulation. Glia 62:1713-1723.

Meek J, Yang JY, Han VZ, Bell CC. 2008. Morphological analysis of the mormyrid cerebellum using immunohistochemistry, with emphasis on the unusual neuronal organization of the valvula. J Comp Neurol 510:396-421.

Mikami Y, Yoshida T, Matsuda N, Mishina M. 2004. Expression of zebrafish glutamate receptor delta2 in neurons with cerebellum-like wiring. Biochem Biophys Res Commun 322:168-176.

Mikoshiba K. 2015. Role of IP3 receptor signaling in cell functions and diseases. Advances in biological regulation 57:217-227.

Minaki Y, Nakatani T, Mizuhara E, Inoue T, Ono Y. 2008. Identification of a novel

transcriptional corepressor, Corl2, as a cerebellar Purkinje cell-selective marker. Gene Expr Patterns 8:418-423.

Miyasaka N, Knaut H, Yoshihara Y. 2007. Cxcl12/Cxcr4 chemokine signaling is required for placode assembly and sensory axon pathfinding in the zebrafish olfactory system. Development 134:2459-2468.

Miyata T, Maeda T, Lee JE. 1999. NeuroD is required for differentiation of the granule cells in the cerebellum and hippocampus. Genes Dev 13:1647-1652.

Miyata T, Ono Y, Okamoto M, Masaoka M, Sakakibara A, Kawaguchi A, Hashimoto M, Ogawa M. 2010. Migration, early axonogenesis, and Reelin-dependent layer-forming behavior of early/posterior-born Purkinje cells in the developing mouse lateral cerebellum. Neural Dev 5:23.

Nakatani T, Minaki Y, Kumai M, Nitta C, Ono Y. 2014. The c-Ski family member and transcriptional regulator Corl2/Skor2 promotes early differentiation of cerebellar Purkinje cells. Dev Biol 388:68-80.

Nakayama M, Nakajima D, Yoshimura R, Endo Y, Ohara O. 2002. MEGF1/fat2 proteins containing extraordinarily large extracellular domains are localized to thin parallel fibers of cerebellar granule cells. Mol Cell Neurosci 20:563-578.

Nieuwenhuys R, Pouwels E, Smulders-Kersten E. 1974. The neuronal organization of cerebellar lobe C1 in the mormyrid fish Gnathonemus Petersii (teleostei). Zeitschrift fur Anatomie und Entwicklungsgeschichte 144:315-336.

Ogata H, Goto S, Sato K, Fujibuchi W, Bono H, Kanehisa M. 1999. KEGG: Kyoto Encyclopedia of Genes and Genomes. Nucleic acids research 27:29-34.

Pouwels E. 1978. On the development of the cerebellum of the trout, Salmo gairdneri. IV. Development of the pattern of connectivity. Anat Embryol (Berl) 153:55-65.

Qin Z, Raymond PA. 2012. Microarray-based gene profiling analysis of Muller glia-derived retinal stem cells in light-damaged retinas from adult zebrafish. Methods in molecular biology 884:255-261.

Rabe TI, Griesel G, Blanke S, Kispert A, Leitges M, van der Zwaag B, Burbach JP, Varoqueaux F, Mansouri A. 2012. The transcription factor Uncx4.1 acts in a short window of midbrain dopaminergic neuron differentiation. Neural Dev 7:39.

Reimand J, Arak T, Vilo J. 2011. g:Profiler--a web server for functional interpretation of gene lists (2011 update). Nucleic acids research 39:W307-315.

Reimand J, Kull M, Peterson H, Hansen J, Vilo J. 2007. g:Profiler--a web-based toolset for functional profiling of gene lists from large-scale experiments. Nucleic acids

research 35:W193-200.

Ristori E, Nicoli S. 2015. miRNAs expression profile in zebrafish developing vessels. Methods in molecular biology 1214:129-150.

Robinson MD, McCarthy DJ, Smyth GK. 2010. edgeR: a Bioconductor package for differential expression analysis of digital gene expression data. Bioinformatics 26:139-140.

Sasagawa Y, Nikaido I, Hayashi T, Danno H, Uno KD, Imai T, Ueda HR. 2013. Quartz-Seq: a highly reproducible and sensitive single-cell RNA sequencing method, reveals non-genetic gene-expression heterogeneity. Genome biology 14:R31.

Sato A, Sekine Y, Saruta C, Nishibe H, Morita N, Sato Y, Sadakata T, Shinoda Y, Kojima T, Furuichi T. 2008. Cerebellar development transcriptome database (CDT-DB): profiling of spatio-temporal gene expression during the postnatal development of mouse cerebellum. Neural networks : the official journal of the International Neural Network Society 21:1056-1069.

Schuller U, Kho AT, Zhao Q, Ma Q, Rowitch DH. 2006. Cerebellar 'transcriptome' reveals cell-type and stage-specific expression during postnatal development and tumorigenesis. Mol Cell Neurosci 33:247-259.

Storey JD. 2003. The positive false discovery rate: a Bayesian Interpretation and the q-value. Ann Stat 31:2013-2035.

Stuckenholz C, Lu L, Thakur P, Kaminski N, Bahary N. 2009. FACS-assisted microarray profiling implicates novel genes and pathways in zebrafish gastrointestinal tract development. Gastroenterology 137:1321-1332.

Suzuki R, Shimodaira H. 2006. Pvclust: an R package for assessing the uncertainty in hierarchical clustering. Bioinformatics 22:1540-1542.

Takeuchi M, Matsuda K, Yamaguchi S, Asakawa K, Miyasaka N, Lal P, Yoshihara Y, Koga A, Kawakami K, Shimizu T, Hibi M. 2015a. Establishment of Gal4 transgenic zebrafish lines for analysis of development of cerebellar neural circuitry. Dev Biol 397:1-17.

Takeuchi M, Yamaguchi S, Yonemura S, Kakiguchi K, Sato Y, Higashiyama T, Shimizu T, Hibi M. 2015b. Type IV Collagen Controls the Axogenesis of Cerebellar Granule Cells by Regulating Basement Membrane Integrity in Zebrafish. PLoS genetics 11:e1005587.

Takeuchi T, Ohtsuki G, Yoshida T, Fukaya M, Wainai T, Yamashita M, Yamazaki Y, Mori H, Sakimura K, Kawamoto S, Watanabe M, Hirano T, Mishina M. 2008.

Enhancement of both long-term depression induction and optokinetic response adaptation in mice lacking delphilin. PLoS One 3:e2297.

Tam WY, Leung CK, Tong KK, Kwan KM. 2011. Foxp4 is essential in maintenance of Purkinje cell dendritic arborization in the mouse cerebellum. Neuroscience 172:562-571.

Tanabe K, Kani S, Shimizu T, Bae YK, Abe T, Hibi M. 2010. Atypical protein kinase C regulates primary dendrite specification of cerebellar Purkinje cells by localizing Golgi apparatus. J Neurosci 30:16983-16992.

Thisse C, Thisse B. 1998. High Resolution Whole-Mount in situ Hybridization. Zebrafish Science Monitor. Vol 5.

Trapnell C, Williams BA, Pertea G, Mortazavi A, Kwan G, van Baren MJ, Salzberg SL, Wold BJ, Pachter L. 2010. Transcript assembly and quantification by RNA-Seq reveals unannotated transcripts and isoform switching during cell differentiation. Nat Biotechnol 28:511-515.

Uemura T, Lee SJ, Yasumura M, Takeuchi T, Yoshida T, Ra M, Taguchi R, Sakimura K, Mishina M. 2010. Trans-synaptic interaction of GluRdelta2 and Neurexin through Cbln1 mediates synapse formation in the cerebellum. Cell 141:1068-1079.

Uesaka N, Uchigashima M, Mikuni T, Nakazawa T, Nakao H, Hirai H, Aiba A, Watanabe M, Kano M. 2014. Retrograde semaphorin signaling regulates synapse elimination in the developing mouse brain. Science 344:1020-1023.

Volkmann K, Chen YY, Harris MP, Wullimann MF, Koster RW. 2010. The zebrafish cerebellar upper rhombic lip generates tegmental hindbrain nuclei by long-distance migration in an evolutionary conserved manner. J Comp Neurol 518:2794-2817.

Wang W, Crandall JE, Litwack ED, Gronostajski RM, Kilpatrick DL. 2010. Targets of the nuclear factor I regulon involved in early and late development of postmitotic cerebellar granule neurons. J Neurosci Res 88:258-265.

Wang W, Mullikin-Kilpatrick D, Crandall JE, Gronostajski RM, Litwack ED, Kilpatrick DL. 2007. Nuclear factor I coordinates multiple phases of cerebellar granule cell development via regulation of cell adhesion molecules. J Neurosci 27:6115-6127.

Wingate R. 2005. Math-Map(ic)s. Neuron 48:1-4.

Wingate RJ. 2001. The rhombic lip and early cerebellar development. Curr Opin Neurobiol 11:82-88.

Wingate RJ, Hatten ME. 1999. The role of the rhombic lip in avian cerebellum development. Development 126:4395-4404.

Wullimann MF, Grothe B. 2014. The Central Nervous Organization of the Lateral Line System. In: Coombs S, Bleckmann H, Fay RR, Popper AN, eds. The lateral line system. Vol 48. Springer Handbook of Auditory Research. Heidelberg-New York: Springer. p 195-251.

Yamasaki T, Kawaji K, Ono K, Bito H, Hirano T, Osumi N, Kengaku M. 2001. Pax6 regulates granule cell polarization during parallel fiber formation in the developing cerebellum. Development 128:3133-3144.

Yoshida M, Hirano R. 2010. Effects of local anesthesia of the cerebellum on classical fear conditioning in goldfish. Behav Brain Funct 6:20.

Zervas M, Millet S, Ahn S, Joyner AL. 2004. Cell behaviors and genetic lineages of the mesencephalon and rhombomere 1. Neuron 43:345-357.

Zhao R, Lawler AM, Lee SJ. 1999. Characterization of GDF-10 expression patterns and null mice. Dev Biol 212:68-79.

Zupanc GK, Hinsch K, Gage FH. 2005. Proliferation, migration, neuronal differentiation, and long-term survival of new cells in the adult zebrafish brain. J Comp Neurol 488:290-319.

Figure Legends

Figure 1. Cell sampling and RNA-seq method.

A-E: Expression of Venus or GFP in the brain of 14-dpf aldoca:GAP-Venus (A), gSA2AzGFF152B; UAS:GFP (152B; UAS:GFP) (B), hspzGFFgDMC156A; UAS:GFP (156A; UAS:GFP) (C), hspGFFDMC28C; UAS:GFP (28C; UAS:GFP) (D), SAGFF(LF)251A; UAS:GFP (251A; UAS:GFP) (E), and control zebrafish larvae (F). Dorsal views. Scale bars: 200 μm in Fig. 1A-F. About five larval brains from each line were analyzed. Representative data are shown. White arrows indicate the GAP-Venus- or GFP-expressing cells that were collected by FACS. **G:** Sample preparation procedure for RNA-seq. WTA: whole transcriptome amplification. **H, I:** FACS-mediated isolation of GFP/Venus+ cells from Tg lines. FACS data for gSA2AzGFF152B; UAS:GFP (granule cells) (H). FACS data for aldoca:GAP-Venus (Purkinje cells) (I). GFP/Venus^{+} cells were isolated through four successive FACS gates. Gate 1: SSC-A (side scatter area) and FSC-A (forward scatter area). Gate 2: FSC-W (forward scatter-width) and FSC-H (forward scatter-height). Gate 3: SSC-W (side scatter-width) and SSC-H (side scatter-height). Gate 4: FITC-A. Cells expressing high levels of GFP/Venus were sorted. The cell populations selected with Gate 4, 3, 2, and 1 are sequentially labelled with green, dark blue, sky blue, and red dots. The cell population removed with Gate 1 is labelled with black dots. **J:** Hierarchical clustering of cerebellar neural cells based on expression profiles. Transcriptome clustering analysis using RNA-seq data from the Tg lines gSA2AzGFF152B; UAS:GFP (152B, for granule cells), aldoca:GAP-Venus (aldoca, for Purkinje cells), hspzGFFgDMC156A; UAS:GFP (156A, for eurydendroid cells), and SAGFF(LF)251A; UAS:GFP (251A, for Bergmann glial cells). Values at

each edge represent p-values of approximately unbiased test (red) and bootstrapping probability (green) for supporting the bifurcation. See the manual of pvclust for details (https://cran.r-project.org/web/packages/pvclust/).

Figure 2. Expression of granule-cell genes at the early larval stage (5 dpf).
A: *vglut1* expression in granule cells at 5 dpf. Dorsal (left) and lateral (right) views with illustrations showing the location of granule cells (magenta circles). **B**: Transcription regulators: *neurod*, *tlx3a*, *nfia*, *prdm8b*, *neurod2*, *uncx4.1*, *pax6a*, *neurod6b*, *tlx3b*, and *neurod6a*. Figures in each category (B-F in Figure 2-4) are arranged in order of expression level. For some genes, expression in granule cells is marked by arrowheads. Scale bars: 200 μm. Five to ten larvae were stained with each probe. Representative data are shown (Fig. 2-4).

Figure 3. Expression of granule-cell genes at the early larval stage (5 dpf).
A: Genes related to intercellular signaling and synapse formation: *cspg5b*, *cbln12*, *reelin*, *wu:fj39j12*, *fgf8a*, and *fat2*. **B**: Genes related to cytoplasmic signaling and calcium: *dusp5*, *dlg1*, *mapk11*, *camk4*, and *camkk2*. Expression in granule cells is marked by arrowheads. Scale bars: 200 μm.

Figure 4. Expression of granule-cell genes at the early larval stage (5 dpf).
A: Metabolism: *dpysl5b*. **B:** Other: *ndrg3b*. Expression in granule cells is marked by arrowheads. Scale bars: 200 μm.

Figure 5. Expression of granule-cell genes in regions of the adult cerebellum.

A-D: Expression of *neurod*, *cbln12*, *fat2*, and *wu:fj39g12* in sagittal sections of the adult tectum, cerebellum, and dorsal hindbrain. CC: crista cerebellaris; GCL: granule-cell layer; LCa: lobes caudalis cerebelli; ML: molecular layer; MON: medial octavolateralis nucleus; TL: torus longitudinalis. Scale bars: 400 μm in A (applies to A–D). Multiple sections from two or more adult fish brains were stained with each probe. Representative data are shown.

Figure 6. Expression of Purkinje-cell genes at the early larval stage (5 dpf).

A: *aldoca* expression in Purkinje cells at 5 dpf. Dorsal (left) and lateral (right) views with illustrations showing the location of Purkinje cells (magenta circles). **B**: Transcription regulators: *ebf3*, *skor1b*, *foxp1b*, *skor2*, *foxp4*, *rorb*, *znf385c*, and *pbxip1b*. For some genes, expression in Purkinje cells is marked by arrowheads. Scale bars: 200 μm in Fig. 6A. Five to ten larvae were stained with each probe. Representative data are shown (Fig. 6-10).

Figure 7. Expression of Purkinje-cell genes at the early larval stage (5 dpf).

Intercellular signaling and synapse formation/function: *grm1a*, *lingo4b*, *kcnj3a*, *plxdc1*, *itpr1b*, and *sema7a*. Expression in Purkinje cells is marked by arrowheads. Scale bar: 200 μm.

Figure 8. Expression of Purkinje-cell genes at the early larval stage (5 dpf).

A: Cytoplasmic signaling and calcium-related: *pvalb7*, *rgs3a*, *casq2*, *lmo1*, *gnaq*, *pvalb6*, *atp2a*, *camk2dl*, *camkvl*, and *grid2ipa*. **B:** Cytoskeleton: *ssx2ipb* and *phactr4b*. Expression in Purkinje cells is marked by arrowheads. Scale bar: 200 μm.

Figure 9. Expression of Purkinje-cell genes at the early larval stage (5 dpf). Metabolism: *ca8*, *pfkfb3*, *gad1b*, *dgkh*, and *gad2*. Scale bar: 200 μm.

Figure 10. Expression of Purkinje-cell genes at the early larval stage (5 dpf). Others: *C15H11orf87*, *dazap1*, *mpped1*, *dnajb6b*, *st6galnac5b*, *nhsl1a*, and *trim66*. Expression in Purkinje cells is marked by arrowheads. Scale bar: 200 μm.

Figure 11. Expression of Purkinje-cell genes in the adult cerebellum and cerebellum-like structures. **A-J**: Expression of *pvalb7*, *aldoca*, *hpca*, *C15H11orf87*, *rgs3a*, *ca8*, *grm1a*, *lingo4b*, *itpr1b*, and *grid2ipa*, in sagittal sections of the adult tectum, cerebellum, and dorsal hindbrain. Aa and Ab show magnified views of the regions outlined in A; Ja and Jb show magnified views of the regions outlined in J. Arrowheads indicate type I neurons in the optic tectum (Aa and Ja) and crest cells in the dorso-anterior hindbrain (Ab and Jb). MON: medial octavolateralis nucleus; PCL: Purkinje-cell layer; TeO: optic tectum. Scale bars: 400 μm in A (applies to A–J); 200 μm in Aa (applies to Aa, Ab, Ja, and Jb). Multiple sections from two or more adult fish brains were stained with each probe. Representative data are shown.

Figure 12. Expression of Bergmann glial genes at 5 dpf and in the adult brain.

A: Expression of *gdf10a*, *gdf10b*, and *grik2* at 5 dpf, showing dorsal and lateral views.

B: Expression of *grik2* in the adult brain. Scale bars: 200 μm in A; 400 μm in B. Five to ten larvae (A) or multiple sections from two or more adult fish brains were stained with each probe. Representative data are shown.

Supplemental Information

Supplementary Tables

Suppl. Table 1. Genes expressed in Venus/GFP-expressing cells from Tg larvae

Excel file: Supplementary Table1.xls

Suppl. Table 2. Granule-cell genes

Excel file: Supplementary Table2.xls

Suppl. Table 3. Purkinje-cell genes

Excel file: Supplementary Table3.xls

Table 1. PCR primers for isolating riboprobes

Gene symbol	Oligo1	Oligo2
ndrg3b	CCGGATCCCACACAGACCAGTTCACAGA	CCAAGCTTGCACAGAAAACGAAGCAGTG
cbln12	CCGGATCCGGCTCCATACGATAACGCTA	CCAAGCTTGGTAAGCCTTGTCTCCTCTT
scg2b	CCTCCTCCATACACTAACTG	GGTGTACTGCTCGTCCAAATC
dlg1	CCGGATCCGAGACAGAAAGATGCTCAGC	CCAAGCTTGAATGACATCTGCCTGCTTC
wu:fj39g12	CCATGCTCCTGTGTTTGAGT	CCTAAGTAGGACAACAGTCAT
mapk11	GGAAGCTTGCAAGGATCGCACAATGGA	CCGGTACCCCCACTCTGTCCAACATTGT
rasd1	GGGGATCCCGTCGGAAAACGAGTTTGAC	CCAAGCTTGGAACATCTGATCCACGTTC
tlx3a	CTGTGCTTCCCCTGGATGGACA	TTGCGGTTCTCTCCTGAGCC
prdm8b	CCGGATCCCTTGAGCTCCAGCAGAAATC	CCAAGCTTGATGACTTCTTGACCTCGGT
neurod2	GCAAAGGACTATCCCAGCC	CCTAACTGTGGAAAAAGGCG
dpysl5b	CGTCTTCATGTGTGCTCAG	GGATGCGACTCTGATTGTG
apba1b	CCGATGCAGAAAGCCAAGG	GGATAAGTCCTCAACTTCGTTC
nebl	CGACTGAGACAGCAAAGTGA	CCATCCCGAAATGACACCT
cxcl14	GGGGATCCCGACACTGTTTGAGGATCTC	GGTGTGCTTTATAAGCTTGTC
neurod6b	GGGGATCCGAGAGAGGAGGACGAGAACG	GGGAATTCAGGACTCGTAGGACGCGTAA
pcdh10a	CTCAATCTTGGATGGAGGG	CGGTGATGTCAGTCTCTGG
uts1	CCTGCTCATCACTTCAGTC	CCTCGTCGAGGTATTTGCG
myt1b	GGGAAACTCCTGAACCAGC	CCTCTTCTTCTGTATTGGTG
mstnb	GCTGTGTTCCACATGTGAGT	GCCAAGTCGTTTCCCTTCG
si:dkey-100n10.2	CCACAACACATTTGAGGTGC	GGTCTGCGTTCATTCTGCG
cbln2b	CCTGATGCAGAACGAATACCC	CCATAAAGCACTTCCGCAGC
oprd1b	GCACTCGCATAGAGCAGAA	CCCACAATTCCCACAATTCC
neurod6a	CCCGGACGTTCAATCGCACATGT	CCCCCTAAACAGTGCCCTGTGTA
fat2	GGGGATCCCCTCACTGTTGAGGCTACA	CCAAGCTTCCATCATAAAAGGCTGAGGG
uncx4.1	CCAATTTGGAGGCTCTTTGG	GGCTAAGAGCTTGTTCTGAG
camk4	CCCATATGGACACTGCTCA	GGTACGGTTCAGTATCTTTCT
dusp5	GGGGATCCGGTCTCCAGCATAGATTGC	CCAAGCTTGGTACAGGAAAGGCAAGAT
nfia	GGGGATCCCCTGTACTTGGCCTACTTCG	CCAAGCTTGGAAATGAAGACTTGACGGC
dacha	CGATGCAGGACAGCTCTCG	GGATGGGAAGAGGGCTGTG
cspg5b	CCGGATCCCTCTAGGCGCACGTTGTTTT	CCAAGCTTGATCTCCAGTTGAGGAGAAG
gabrd	CCCCAGATTTCCACGTCTTAGCC	CCCCAGCATTTCTTCTCCTCGCT
camkk2	CCCCTTGGTTAGGACGATGTTGC	CCCGTCTCTCTCCCTAAACTCTC
hpca	CTGAGGATGAATCCACACCA	GTGCCCTCACAAAACAAAGG
C15H11orf87	GGGGATCCAGAGACTGGCGCTTTCCAT	GGGAATTCCAAGACACAGCGACCGATT
ebf3	CCTTTGCTCCAGTTGTCAGG	GCACATCGGTGAAAGAGAAAC
dazap1	GAGATGAAATCGGGAAGCTG	CCATGATGTCGTGAAAATGC
mpped1	GGGGATCCGCCGGAGAACTATGAAAACG	GGGAATTCTCATGAGCTCCGGGGATT
skor1b	CACGGCAATAAACACACGAC	GACGGGGAGTCAGCATCTTA
grm1a	GAGGAGGGTTCAGAAATGGA	CTCATTTGCCAGCATGTTTC
tfap2a	CCTTCCGATCTTGGCATTTA	CACTAAAACAGGAGGCACCA
casq2	CCTGGCCAGTGCTAAGAAAG	GTTCAGCTGCCTCTTGGAAA
foxp1b	GGACCGTTGACGAGCTAGAG	CCAGTCTTGGGCTTGCTATA
lmo1	GGGGATCCAGACAAGGAAGAGGGTGTGC	GGGAATTCTTGAACTTGCGTCTCAAAGC
gnaq	CGTTAACACGGGAGGAACAC	GAGCTGTCGGTCGATCTCAT
lingo4b	CGAGGATGATGTTAGAGGAC	CCTGAAATGTTTCCACCTCA
skor2	GGGGATCCCCTCACAGAAAGCCCATCTC	GGGAATTCGCTTGGGAAGGAGGCTAGTT
pvalb6	GAGCAGCATCCTCAACCATG	GTGTGTGATGGGGTGATGTT
ptpreb	CAGCAGCAATCTGGAAACAA	GGAAGCAAGCTGTCGGATAA
ssx2ipb	GGGGATCCAGGGTATCATTGCGAGTCGT	GGGAATTCGCTTGAGTTTCCTCCACTGC
foxp4	GCTACAGCAGCAACACATTC	GCGTGTTCACTATTCAGGTG
kctd4	GGGGATCCGTGAGGAACGGAATGGAATG	GGGAATTCCTCGATGAAGGTGTTGTCGC
atp2a3	GGGGATCCGGCCATAATCCTTTCCCTGT	GGGAATTCGACACACAACGGCTTGACAT
camk2d1	GTCACAACAGTGCGAGTCAG	CTGGCATCAGCCTCACTGTA

dgkh	CCCAAACACAGCTGTCCTG	CCAGGTCAGGATCTATGAATG
kcnj3a	GGGGATCCCAACAGCCACATGGTTTCAG	GGGAATTCTAGGCAGTCAAGGGAGCTGT
dnajb6b	ACAAAAACCCCAATGACAAAGAGGA	CGTTTAGTGGTGATCCTCTTTCCGT
plxdc1	GGGGATCCTGCAAGCAATGTCTCCAGTC	GGGAATTCCATAGCTGGAATGGCATCCT
rorb	CGCACTCTTACGAGGAGGTC	GTGTGCAGAGTGCAGAGAGC
dgkaa	CACTGTCCTGCAGACCTCAA	CAGGCCTCAGTTCAGACACA
znf385c	CCCTTCGTGTAAAAGCAAGC	GCGATCAATAGGGGGAGAAT
tnc	CCTCTATGGCAGTGGCTGTT	CCACTGCAGTAGGGTTTGGT
st6galnac5b	CATTCGTATGAATGATGCCCCAAC	TGCATTCATCCGTGCCCGAA
rftn2	CTATGTGAGCTGCCTCATGC	GTAACAGCAGGCCAACGAAT
lmo7a	CAAGATCAAACCTGGCATCA	CAGCGAATTGAGGCTGTCTA
cuedc1a	CCTAGCATGGAGCATGAGGT	GCTCGTCCTCCAAGTACTGC
nhsl1a	TTAATGCTAGCGGAGAAGCTGTGG	GTGCGCGAGCGCCCATATTT
lrrfip1a	CCAGCAAAAATGGGTTGACT	GCGAGACCTTTTGCTCTCAT
pbxip1b	GGGAGGGAAAGAGGAGAGAAGTGG	CCGGAGGTTTTGTCTGGAGGTATGT
dgkzb	GATAATCCAGGTTGGAGGGA	GCTCAATCCGGCACAATAAT
trim66	CAGTCCATAGCTGCTCGCATTGG	TGGATGTCGTGATACGAGGATCTTG
itpr1b	GGGGATCCGAACTCGGTGAACTGCAACA	GGGAATTCCATCAGGCACAGACACCAGT
sema7a	AATTGAAGAAGTGATCGGCCCG	TGCAGTTGTCTTTCTCCCAGCG
grid2ipa	GGGGATCCCAGCATCGGAGTCGTGTCTA	GGGAATTCGCCTGTGCTTCTTAGGGATG
rgs3a	GAACCGACTAGCTTTCCTGAGGAGG	TGATGTCGATGTGGTGCTTGGTT
camkvl	GGCGAAAGAATTTTGTGAGC	GCCCAACAATCAACTGGTCT
phactr4b	GGGGATCCCACCTGTCACAAAACGCAAC	GGGAATTCGGGTGCTGATCTTCCTCATC
pfkfb3	AGGGAGAGGTTTCCCGAGGAGTTTT	TGGACAGAGCCAGTGTGGTGTGTG
camk2d2	CGCATCATCATCCTCTTCCT	CTCAATGGCCAAACCAAAGT
r3hdm1	GGGGATCCGCCCATCTGGCTAATCTGAA	GGGAATTCCGGTTTGGTAGGCTCAGTGT
Grik2 (CR933820.2)	CCGGATCCCAGAATCAGCAACATGTTGGG	CCAAGCTTCTGTGCAGAAGAGTGAAGTG
gdf10a	GCCATTTCAGAGCCCAACAGTG	TGGTTGCATGGTTGGACGGG
gdf10b	AGCATTTACCTCCTCACAACATGCC	CGCATGATTGGATGGATGGACA
rrm2	GAGAGGGAATTTTTGTTCAATGCCA	CCTCCAACGAAATGTTCTCCATGAA
CD200	GTGGAAGAAAACAGCTGAGCAAGG	CGACACATATATGGCTGCCTCAAGA

The PCR primers used to isolate cDNA fragments. The restriction enzyme sites used for subcloning are underlined.

Table 2. Quantities of Tg larvae, isolated cells, and total RNA, and the number of sequence reads

Tg line	Sample No.	Cell type	Number of larvae	Number of cells	RNA (ng)	Number of raw reads	Number of reads after trimming
152B	1	granule cells	123	50,000	5.0	9,447,709	8,613,847
152B	2		241	144,393	44.1	9,888,278	9,044,879
aldoca	1	Purkinje cells	200	53,173	36.9	9,901,381	8,723,831
aldoca	2		156	31,190	15.2	9,163,903	8,104,385
aldoca	3		80	15,000	38.0	9,563,904	8,506,632
156A	1	eurydendroid cells	85	6,220	38.6	10,656,761	9,056,682
156A	2		51	3,846	20.3	10,169,748	8,996,658
28C	1	Inferior olive nucleus	37	11,000	42.0	9,563,380	8,294,339
28C	2		29	1,500	7.7	9,708,160	8,630,867
28C	3		50	1,825	104.8	9,816,689	8,463,464
251A	1	Bergmann glial cells	141	38,480	14.0	10,069,067	8,971,575
251A	2				28.7	10,100,861	8,723,426

The Tg lines gSA2AzGFF152B; UAS:GFP (152B, for granule cells), aldoca:GAP-Venus (aldoca, for Purkinje cells), hspzGFFgDMC156A; UAS:GFP (156A, for eurydendroid cells), hspGFFDMC28C; UAS:GFP (28C, for IO neurons), and SAGFF(LF)251A; UAS:GFP (251A, for Bergmann glial cells) were used to isolate GFP/Venus^{+} cells by FACS. The number of larvae used, the number of cells, and the amount of RNA isolated are indicated for each line. Regarding sequencing, the number of raw reads and number of reads after quality control are also indicated. For 251A, isolated GFP^{+} cells were divided into two samples that were analyzed by RNA isolation and RNA-seq.

Table 3. Expression levels of selected marker genes in RNA-seq data

Tg lines	152B		aldoca			156A		28C			251A	
Sample No.	1	2	1	2	3	1	2	1	2	3	1	2
(A) Granule-cell marker genes												
*slc17a7**	6.3	4.2	0.0	0.0	0.0	0.0	0.0	0.0	0.0	0.0	0.2	0.0
neurod	1544.6	1673.4	20.2	18.4	16.1	203.4	152.6	60.5	124.5	41.7	134.2	160.9
reelin (reln)	564.1	373.0	11.3	5.4	8.6	14.9	22.8	38.8	28.3	10	69.7	46.7
(B) Purkinje-cell marker genes												
aldoca	6.6	2.1	1808.4	1586.0	2443.4	46.1	11.2	35	340.6	1.0	40.6	39.3
parvalbumin 7	2.4	4.0	1091.8	1138.6	1094.9	7.7	6.1	17.3	58.5	228.1	26.6	27.7
ca8‡	4.9	3.7	731.4	741.3	807.9	1.2	7.4	7.1	82.3	5.5	26.4	32.5
lhx1a	189	147.1	766.2	759.8	525.9	26.4	55.6	154.2	116.4	61.7	31.7	34.4
gad1b	10.9	5.2	404.8	299.8	433.2	9.9	12.5	179.2	133.5	7.3	34.5	45.7
(C) Eurydendroid genes												
olig2	5.6	8	4.8	1.6	0.4	101.8	59.4	20	31.4	5.7	18.5	13.4
slc17a6b§	54.3	38.1	5.4	3.7	1.1	44.5	68.2	33.4	26.4	7.3	16.7	17.4
(D) Inferior olive genes												
hoxb5a	0.9	0.9	2.0	0.9	0.2	2.6	0.8	59.2	74.2	47.3	2.5	2.8
pou4f1	0.4	0.9	4.5	2.6	2.5	2.4	2.7	17.1	22.4	3.2	9.7	8.3
(E) Bergmann glia genes												
fabp7a	440.5	590.9	731.1	1247.7	1575.7	1213.6	841.8	160.7	713.1	115.4	1457.3	1474.7

Gene expression levels are shown as FPKM (fragments per kilobase of exon per million mapped fragments) of marker genes. The Tg line gSA2AzGFF152B; UAS:GFP (152B) expresses GFP in granule cells; aldoca:GAP-Venus (aldoca) expresses Venus in Purkinje cells; hspzGFFgDMC156A; UAS:GFP (156A) expresses GFP in eurydendroid cells; and hspGFFDMC28C; UAS:GFP (28C) expresses GFP in IO neurons. The SAGFF(LF)251A; UAS:GFP (251A) line expresses GFP in Bergmann glial cells.

**slc17a7*: vglut1

‡*ca8*: carbonic anhydrase 8

§*slc17a6b*: *vglut2a* is expressed in granule cells, eurydendroid cells, and IO neurons.

Table 4. Enriched GO terms and KEGG pathways for granule cells

Term ID	Type	GO Term	Number	p-value
GO:0007399	BP	nervous-system development	83	2.15E-10
GO:0044700	BP	single organism signaling	166	2.00E-03
GO:0034220	BP	ion transmembrane transport	32	2.35E-02
GO:0051252	BP	regulation of RNA metabolic process	107	2.34E-06
GO:0006355	BP	regulation of transcription, DNA-templated	103	1.25E-05
GO:0065007	BP	biological regulation	313	1.66E-13
GO:0050794	BP	regulation of cellular process	294	3.20E-13
GO:0071944	CC	cell periphery	93	2.90E-05
GO:0045202	CC	synapse	29	5.92E-08
GO:0008021	CC	synaptic vesicle	13	2.19E-06
GO:0005874	CC	microtubule	17	4.83E-02
GO:0030054	CC	cell junction	27	8.14E-03
GO:0001071	MF	nucleic-acid binding transcription factor activity	59	2.89E-02
GO:0005515	MF	protein binding	123	9.64E-05
GO:0005085	MF	guanyl-nucleotide exchange factor activity	18	3.76E-02
KEGG:04914	ke	Progesterone-mediated oocyte maturation	13	2.16E-02
KEGG:04068	ke	FoxO signaling pathway	21	3.07E-04
KEGG:04320	ke	Dorso-ventral axis formation	6	2.61E-02
KEGG:04010	ke	MAPK signaling pathway	27	5.54E-03
KEGG:04330	ke	Notch signaling pathway	9	3.22E-02

1075 granule-cell genes were annotated to the following gene ontology (GO) groups: Biological Processes (BP), Cellular Component (CC), and Molecular Function (MF). 1070 granule-cell genes were annotated to the KEGG pathways. The number of genes annotated to each GO term or KEGG pathway and the p-values are indicated.

Table 5. Enriched GO terms and KEGG pathways for Purkinje cells

Term ID	Type	GO Term	Number	p-value
GO:0060322	BP	head development	6	6.86E-03
GO:0006811	BP	ion transport	62	4.47E-07
GO:0048705	BP	skeletal system morphogenesis	14	2.05E-02
GO:0044700	BP	single organism signaling	144	5.79E-03
GO:1990351	CC	transporter complex	15	8.25E-03
GO:0016020	CC	membrane	231	1.56E-05
GO:0004683	MF	calmodulin-dependent protein kinase activity	5	1.68E-02
GO:0015075	MF	ion transmembrane transporter activity	51	6.39E-04
KEGG:04020	ke	Calcium signaling pathway	27	2.51E-04
KEGG:04260	ke	Cardiac-muscle contraction	16	5.07E-05
KEGG:04916	ke	Melanogenesis	16	8.43E-03
KEGG:04070	ke	Phosphatidylinositol signaling system	13	4.07E-03
KEGG:04261	ke	Adrenergic signaling in cardiomyocytes	26	3.21E-06
KEGG:04912	ke	GnRH signaling pathway	19	1.35E-05
KEGG:04270	ke	Vascular smooth-muscle contraction	17	1.99E-03
KEGG:04012	ke	ErbB signaling pathway	13	1.95E-02
KEGG:04540	ke	Gap junction	16	2.87E-03

887 Purkinje-cell genes were annotated to the following GO groups: Biological Processes (BP), Cellular Component (CC), and Molecular Function (MF). 865 Purkinje-cell genes were annotated to the KEGG pathways. The number of genes annotated to each GO group or KEGG pathway and the p-values are also indicated.

Table 6. Genes upregulated in granule cells

Gene ID	Gene symbol	Product	Q-value	152B/ aldoca	FPKM: 152B	FPKM: aldoca
ENSDARG00000019566	neurod1	Neurogenic differentiation	1.13E-72	88.3	1609.0	18.2
ENSDARG00000010052	ndrg3b	Ndrg family 3b	8.79E-40	12.7	862.9	67.9
ENSDARG00000068232	cbln12	Cerebellin 12	3.07E-129	547.6	715.7	1.3
ENSDARG00000038574	scg2b	Secretogranin II, b	7.36E-37	18.6	474.5	25.5
ENSDARG00000077935	reln	Reelin	4.96E-65	55.4	468.6	8.5
ENSDARG00000009677	dlg1	Discs, large homolog1	1.56E-66	74.4	443.0	6.0
ENSDARG00000019013	barhl1b	BarH-like homeobox 1b	1.43E-63	68.4	305.4	4.5
ENSDARG00000043460	wu:fj39g12	Natriuretic peptide precursor C-like	7.58E-72	184.4	275.4	1.5
ENSDARG00000045836	mapk11	MAP kinase 11	1.63E-82	47.3	259.2	5.5
ENSDARG00000019274	rasd1	RAS, dexamethasone-induced	4.32E-45	13.6	259.1	19.0
ENSDARG00000011235	otx2	Orthodenticle homeobox 2	7.42E-30	28.5	240.6	8.4
ENSDARG00000006503	tlx3a	T-cell leukemia homeobox protein 3-like	2.32E-73	2330.3	227.9	0.1
ENSDARG00000054683	prdm8b	PR domain–containing 8b	1.38E-26	22.2	213.6	9.6
ENSDARG00000016854	neurod2	Neurod2	8.79E-58	102	204.1	2.0
ENSDARG00000059311	dpysl5b	dihydropyrimidinase-like 5b	4.04E-54	40.8	180.8	7.9
ENSDARG00000045045	pax6a	Paired box 6a	2.55E-72	100.4	164.2	4.0
ENSDARG00000074328	apba1b	A4 precursor protein–binding family A, 1b	4.23E-43	22.2	158.2	14.2
ENSDARG00000021200	nebl	Nebulette	1.10E-74	102	157. 5	1.6
ENSDARG00000056627	cxcl14	Chemokine (C-X-C motif) ligand 14	1.44E-42	16.8	148.0	8.8
ENSDARG00000020794	neurod6b	Neurogenic differentiation 6b	4.72E-34	39.3	138.3	3.5
ENSDARG00000054274	pcdh10a	Protocadherin 10a	1.41E-24	17.2	132.2	7.7
ENSDARG00000006640	eomesa	Eomesodermin homolog a	2.27E-55	158.4	132.1	0.8
ENSDARG00000017615	tlx3b	T-cell leukemia, homeobox 3b	6.85E-80	241.1	118.1	0.5
ENSDARG00000014927	uts1	Urotensin 1	1.43E-65	78.1	110.4	1.4
ENSDARG00000089464	myt1b	Myelin transcription factor 1b	9.32E-38	11.4	110.0	9.6
ENSDARG00000069133	mstnb	Myostatin b	2.94E-26	10.8	109.0	10.1
ENSDARG00000041959	cxcr4b	Chemokine (C-X-C motif), receptor 4b	7.80E-21	17.7	98.6	5.6
ENSDARG00000062672	si:dkey-100n10.2	G protein–activated inward rectifier potassium channel 1	8.33E-34	78.1	92.6	7.3
ENSDARG00000077151	cbln2b	Cerebellin 2b	9.58E-38	49.1	91.6	1.9
ENSDARG00000071860	nrn1a	Neuritin 1a	1.45E-16	16.2	88.5	5.5
ENSDARG00000037159	oprd1b	Opioid receptor, delta 1b	5.94E-58	124.1	87.9	0.7
ENSDARG00000056915	si:ch211-237l4.6	Unknown	4.64E-36	83.4	84.6	1.0
ENSDARG00000040008	neurod6a	Neurogenic differentiation 6a	6.35E-27	60.9	82.5	1.4
ENSDARG00000090190	bcam	Basal-cell adhesion molecule	3.49E-58	17.6	80.9	4.6
ENSDARG00000068100	si:ch211-240g9.1	Protein FAM19A5-like	7.15E-29	68.1	78,7	1.2
ENSDARG00000010276	ptgs2b	Prostaglandin-endoperoxide synthase 2b	1.25E-19	15.7	77.8	5.0
ENSDARG00000087109	ttc28	Tetratricopeptide repeat domain 28	4.10E-34	18.7	76.5	4.1
ENSDARG00000076244	uo:ion006	Palmdelphinb	1.33E-9	11.9	76.2	6.4
ENSDARG00000027236	rs1a	Retinoschisin 1a	2.81E-21	40.6	75.4	1.9
ENSDARG00000034808	kcnip1b	Kv channel–interacting protein 1b	1.15E-24	12.5	74.3	6.0
ENSDARG00000032049	enah	Enabled homolog	5.23E-33	10.5	70.4	6.7
ENSDARG00000017880	kcnip3b	Kv channel–interacting protein 3b, calsenilin	2.75E-33	74.3	69.3	0.9
ENSDARG00000003399	fgf8a	Fibroblast growth factor 8a	1.22E-50	166.7	65.7	0.4
ENSDARG00000087394	tshz3a	Teashirt zinc finger homeobox 3a	4.45E-34	16.4	64.6	3.9
ENSDARG00000020758	tmem178	Transmembrane protein 178	9.60E-28	47.2	63.6	1.3
ENSDARG00000010878	cdkn1ca	Cyclin-dependent kinase inhibitor 1Ca	8.64E-15	11	63.1	5.8
ENSDARG00000025728	grin1b	Glutamate receptor, ionotropic, NMDA 1b	1.11E-39	42.5	61.5	1.4
ENSDARG00000070781	cx35b	Connexin 35b	9.17E-45	86.1	58.5	0.7

ENSDARG00000010420	ndrg1b	N-myc downstream-regulated 1b	1.34E-31	27.6	57.8	2.1
ENSDARG00000010083	rbfox3	RNA-binding protein, fox-1 homolog 3	9.56E-28	11.2	57.8	5.1
ENSDARG00000097467	si:dkey-22 1l21.2	Unknown	5.23E-12	13.1	57.7	4.4
ENSDARG00000028228	zbtb18	Zinc finger and BTB domain–containing 18	7.50E-34	61.7	55.4	0.9
ENSDARG00000052898	kcnk3b	Potassium channel, subfamily K, member 3b	7.70E-40	155.5	52.5	0.3
ENSDARG00000040123	zfpm2a	Zinc finger protein, FOG family member 2a	7.06E-46	26.2	50.8	1.9
ENSDARG00000042940	nab1a	NGFI-A binding protein 1a	1.61E-17	11.8	47.6	4.0
ENSDARG00000037390	gsg1l	Gsg1-like	8.53E-35	104.4	46.5	0.4
ENSDARG00000061416	C2cd4a	C2 calcium-dependent domain–containing 4A	6.68E-12	14	46.4	3.3
ENSDARG00000041150	slc17a6b	Vglut2a	2.12E-13	13.6	46.2	3.4
ENSDARG00000023886	cacna2d4 b	calcium channel, voltage-dependent, alpha 2/delta subunit 4b	4.40E-40	36.6	46.1	1.3
ENSDARG00000018923	fat2	FAT atypical cadherin 2	2.57E-102	224.5	45.0	0.2
ENSDARG00000087241	ucn3l	Urocortin 3–like	1.29E-7	17.9	43.8	2.45
ENSDARG00000045639	elavl4	ELAV-like neuron-specific RNA- binding protein 4	2.10E-12	10.6	43.3	4.1
ENSDARG00000011555	spag7	Sperm-associated antigen 7	9.67E-8	11.2	42.54	3.8
ENSDARG00000035508	barhl1a	BarH-like homeobox 1a	2.37E-25	26	40.8	1.6

Genes expressed at significantly higher levels in gSA2AzGFF152B; UAS:GFP^{+} cells (152B: granule cells) than in aldoca:GAP-Venus^{+} cells (aldoca: Purkinje cells) (Q-value < 0.01) and shown in Suppl. Table 4. Genes with high variation (more than 4-fold) between the two samples were excluded. Among the granule-cell genes, genes with a fold change > 10 (152B/aldoca) and FPKM > 40 were selected as major granule-cell genes and are listed in this table in descending order of their expression level in 152B (the FPKM: 152B column).

Table 7. Genes upregulated in Purkinje cells

Gene ID	Gene symbol	Product	Q-value	aldoca /152B	FPKM: 152B$^+$	FPKM: aldoca$^+$
ENSDARG00000057661	aldoca	Aldolase C, fructose-biphosphate a	2.11E-43	446.5	4.4	1946
ENSDARG00000018397	hpca	Hippocalcin	6.20E-22	12.3	104.6	1288
ENSDARG00000034705	pvalb7	Parvalbumin 7	5.03E-88	347.7	3.2	1108.4
ENSDARG00000097648	C15H11orf87	C15H11orf87	5.27E-46	87.3	10.8	942.1
ENSDARG00000039098	ca8	Carbonic anhydrase VIII	7.58E-77	176.1	4.3	760.2
ENSDARG00000016300	ebf3	Early B-cell factor 3a	3.74E-32	22.3	32.9	732
ENSDARG00000070846	dazap1	DAZ-associated protein 1	7.77E-37	20	35.2	702.9
ENSDARG00000088181	mpped1	Metallophosphoesterase domain–containing 1	1.23E-50	22.9	30.6	702.4
ENSDARG00000062448	skor1b	SKI family transcriptional repressor 1b	6.60E-65	206.9	3.2	652.3
ENSDARG00000026796	grm1a	Glutamate receptor, metabotropic 1a	5.13E-60	201.6	3.1	616.9
ENSDARG00000059279	tfap2a	Transcription factor AP-2 alpha	4.14E-47	36.6	12.6	461.3
ENSDARG00000008982	casq2	Calsequestrin 2	6.10E-70	457.2	0.9	418.1
ENSDARG00000027419	gad1b	Glutamate decarboxylase 1b	1.95E-46	47	8.1	379.3
ENSDARG00000014181	foxp1b	Forkhead box P1b	3.04E-51	64.2	5.5	355.1
ENSDARG00000034504	lmo1	Lim domain only 1	2.07E-34	16.9	20.2	340.2
ENSDARG00000011487	gnaq	G protein, q polypeptide	8.06E-68	52.3	6.4	333.3
ENSDARG00000078527	lingo4b	Leucine-rich repeat and Ig domain–containing 4b	8.49E-89	778.5	0.4	298.8
ENSDARG00000063614	skor2	SKI family transcriptional repressor 2	1.35E-74	142.2	2.1	297.2
ENSDARG00000009311	pvalb6	Parvalbumin 6	6.40E-67	111.3	2.5	282.7
ENSDARG00000021151	ptpreb	Protein tyrosine phosphatase, receptor type, E, b	5.39E-27	10.7	25.5	272.9
ENSDARG00000061602	ssx2ipb	Synovial sarcoma, X breakpoint 2–interacting protein b	2.79E-82	188.7	1.4	271.8
ENSDARG00000076120	foxp4	Forkhead box P4	4.03E-48	25.8	10	259.4
ENSDARG00000068691	kctd4	Potassium-channel tetramerization domain–containing 4	2.71E-36	14.5	15.6	226.3
ENSDARG00000060978	atp2a3	ATPase, $C2^{++}$ transporting, ubiquitous	3.88E-35	17.6	11.1	194.3
ENSDARG00000043010	camk2d1	CaM kinase II delta 1	4.90E-65	85.6	2.3	194.1
ENSDARG00000018716	dgkh	Diacylglycerol kinase, eta	4.00E-51	21.9	8.7	189.5
ENSDARG00000077165	kcnj3a	Potassium inwardly-rectifying channel, subfamily J, member 3a	4.22E-50	22.7	8.2	186.8
ENSDARG00000020953	dnajb6b	DnaJ homolog, subfamily B, member 6b	4.52E-37	15.4	11.6	178.8
ENSDARG00000078417	plxdc1	Plexin domain–containing1	5.03E-88	1030.9	0.2	177.9
ENSDARG00000015537	gad2	Glutamate decarboxylase 2	7.61E-29	9.1	19.2	175.6
ENSDARG00000033498	rorb	RAR-related orphan receptor B	5.21E-48	54.1	2.9	154.4
ENSDARG00000060626	dgkaa	Diacylglycerol kinase, alpha a	1.20E-44	32.9	4.6	151.3
ENSDARG00000058154	znf385c	Zinc finger protein 385C	3.57E-62	58.2	2.6	149
ENSDARG00000021948	tnc	Tenascin C	3.71E-30	12.8	11.5	146.7
ENSDARG00000057433	st6galnac5b	ST6-N-acetylgalactosaminide alpha-2,6-sialyltransferase 5b	4.92E-67	73.2	2	146.2
ENSDARG00000056078	rftn2	Raftlin family member 2	8.06E-33	9.4	13.7	129
ENSDARG00000004930	lmo7a	LIM domain 7a	1.62E-28	14.9	8.3	123.4
ENSDARG00000023181	pcp4l1	Purkinje-cell protein 4–like 1	6.90E-42	261.4	0.4	117.1
ENSDARG00000068716	cuedc1a	CUE domain–containing 1a	2.56E-52	25.9	4.5	116.5
ENSDARG00000054537	nhsl1a	NHS-like 1a	1.07E-40	13	8.9	115.4
ENSDARG00000030012	lrrfip1a	Leucine-rich repeat interacting protein 1a	1.92E-34	54.1	2	107.5
ENSDARG00000011824	pbxip1b	Pre-B-cell leukemia homeobox interacting protein 1b	1.49E-56	72	1.5	105.7
ENSDARG00000090292	CABZ01071757.1	RALY RNA-binding protein-like	3.19E-30	185.6	0.5	101.4

ENSDARG00000052625	fkbp1b	FK506-binding protein 1b	4.12E-25	14.6	6.9	100.4
ENSDARG00000034229	kcnip3a	Kv channel–interacting protein 3a, calsenilin	1.16E-16	12.3	8.1	99.6
ENSDARG00000074056	kctd1	Potassium-channel tetramerization domain–containing 1	5.39E-27	11.3	8.7	97.7
ENSDARG00000057719	atl2	Atlastin GTPase 2	1.00E-28	10.5	8.9	93.9
ENSDARG00000059775	slc32a1	GABA vesicular transporter, member 1	4.58E-44	16.5	5.5	91.4
ENSDARG00000045760	prmt8b	Protein arginine methyltransferase 8b	3.91E-61	68.7	1.3	87.9
ENSDARG00000087796	ptprmb	Protein tyrosine phosphatase, receptor type, M, b	6.41E-13	42.9	2.0	85.3
ENSDARG00000087176	Sgk494a	Serine/threonine-protein kinase SgK494a	1.59E-65	43.3	1.9	84.5
ENSDARG00000076025	dgkzb	Diacylglycerol kinase, zeta b	2.64E-44	85.7	1	84.2
ENSDARG00000086142	arhgap27	Rho GTPase–activating protein 27	1.00E-34	28.4	2.8	78.7
ENSDARG00000029039	zdhhc23a	Zinc finger, DHHC-type containing 23a	6.50E-24	17.6	4.3	75.6
ENSDARG00000074575	si:ch211-269i23.2	Neurabin-1	2.73E-56	30.3	2.4	71.5
ENSDARG00000002897	b3galt6	UDP-Gal:betaGal beta 1,3-galactosyltransferase polypeptide 6	2.90E-37	15.4	4.6	71.5
ENSDARG00000054332	trim66	Tripartite motif–containing 66	2.45E-77	173.2	0.4	69.3
ENSDARG00000045893	kctd15a	Potassium-channel tetramerization domain–containing 15a	2.05E-54	45.4	1.4	64.5
ENSDARG00000041884	zgc:77147		9.33E-13	15.4	4.2	64.4
ENSDARG00000074275	limch1a	LIM and calponin homology domains 1a	1.76E-37	12.7	4.9	62.1
ENSDARG00000074149	itpr1b	Inositol 1,4,5-triphosphate receptor, type 1b	6.25E-53	51	1.2	60.3
ENSDARG00000027957	fgf12a	Fibroblast growth factor 12a	4.74E-28	42.5	1.3	56.7
ENSDARG00000037921	gng13b	Guanine nucleotide–binding protein, gamma 13b	2.02E-20	23.1	2.4	56.1
ENSDARG00000023683	cacna1fb	Calcium channel, voltage-dependent, L type, alpha 1F subunit	1.92E-31	103.2	0.5	55.7
ENSDARG00000070730	gabra5	GABA A receptor, alpha 5	1.79E-31	25.8	2.1	54.6
ENSDARG00000097718	stard10	StAR-related lipid transfer (START) domain-containing 10	9.22E-10	15.1	3.5	53.1
ENSDARG00000070442	sema7a	Semaphorin 7A	1.58E-43	21.1	2.4	50.6
ENSDARG00000015922	zgc:153952	Serine/threonine-protein kinase 17A	3.65E-14	11.2	4.4	49.4
ENSDARG00000070651	prkcdb	Protein kinase C, delta b	8.04E-36	16.4	2.9	48.4
ENSDARG00000076103	grid2ipa	Grid2-interacting protein, a	5.70E-83	366.3	0.1	48.3
ENSDARG00000007944	lhx1b	LIM homeobox 1b	7.94E-26	19.2	2.5	47.3
ENSDARG00000044718	vav2	Vav2 guanine nucleotide exchange factor	1.08E-38	21.5	2.2	46.5
ENSDARG00000010462	sp9	Sp9 transcription factor	3.71E-17	11.6	3.9	45.5
ENSDARG00000016116	ebf1a	Early B-cell factor 1a	7.03E-37	23.4	1.8	42.5
ENSDARG00000070864	bcl6a	B-cell CLL/lymphoma 6a	8.09E-25	11.6	3.7	42.4

Genes expressed at significantly higher levels in aldoca:GAP-Venus^{+} cells (aldoca: Purkinje cells) than in gSA2AzGFF152B; UAS:GFP^{+} cells (152B: granule cells) (Q-value < 0.01) are shown in Suppl. Table 5. Here, Purkinje-cell genes with a fold change (aldoca/152B) > 10 and FPKM > 40 (aldoca) are shown in descending order of expression level (in the FPKM: aldoca column).

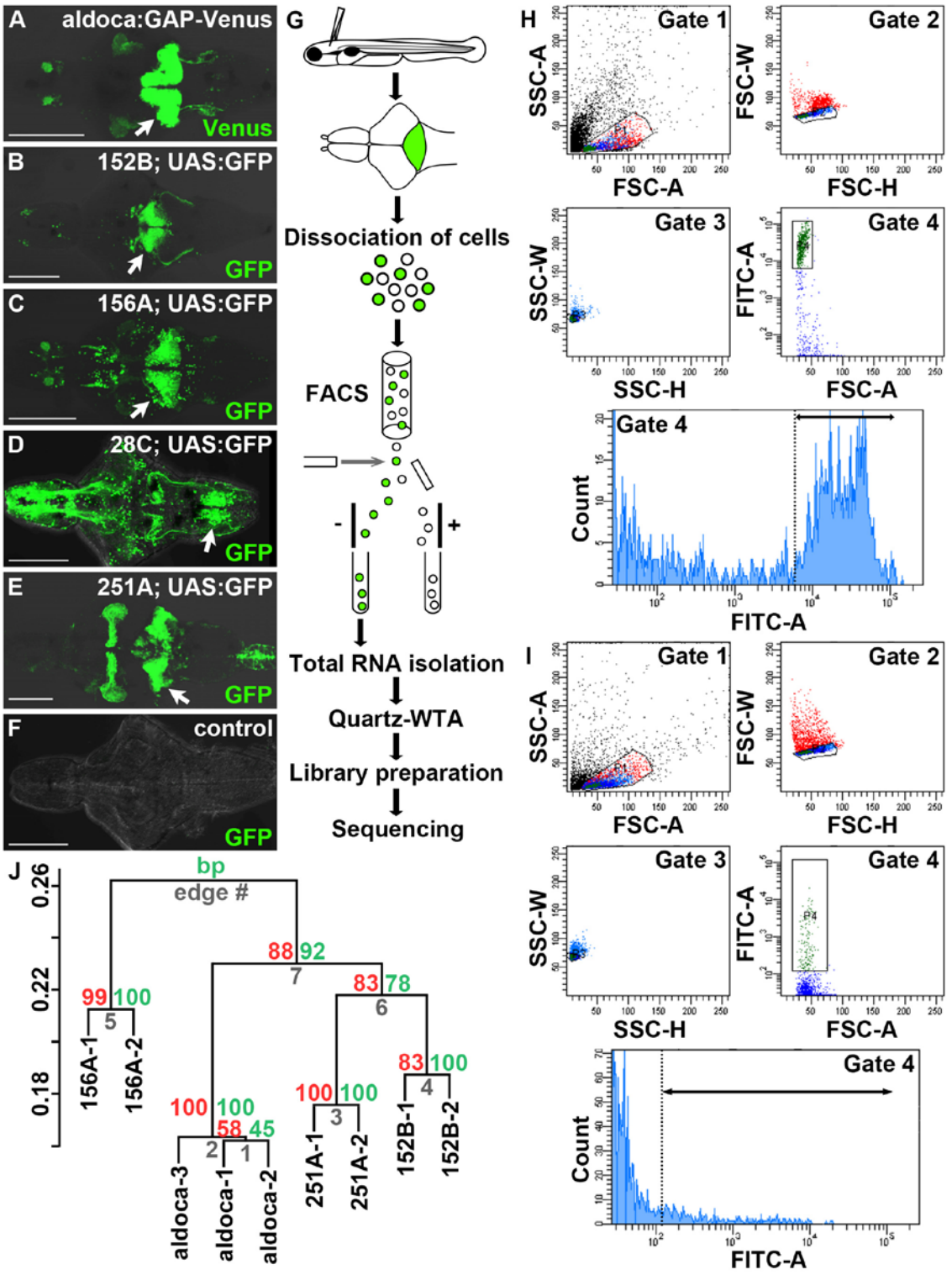

Figure 1. Cell sampling and RNA-seq method.

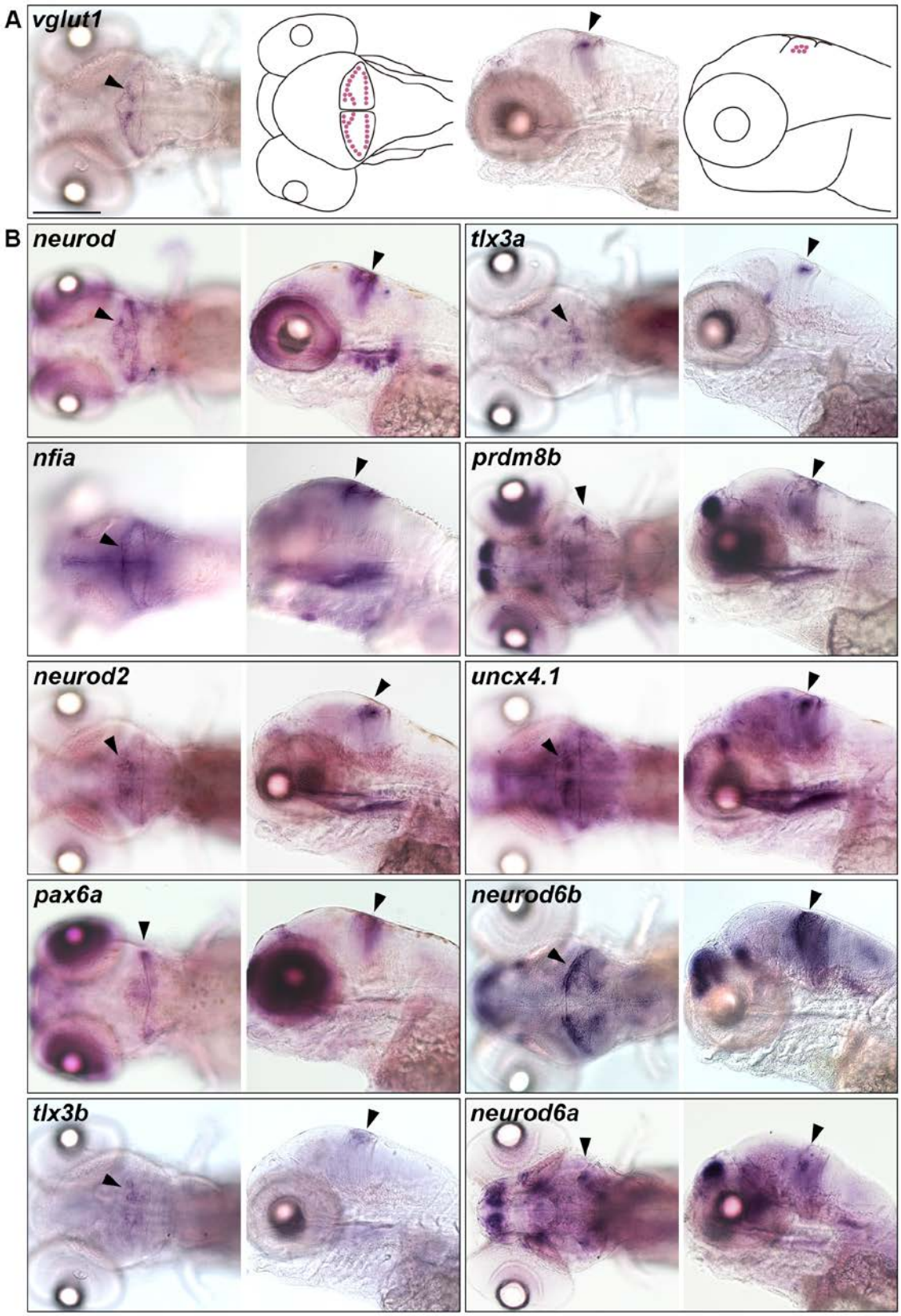

Figure 2. Expression of granule-cell genes at the early larval stage (5 dpf).

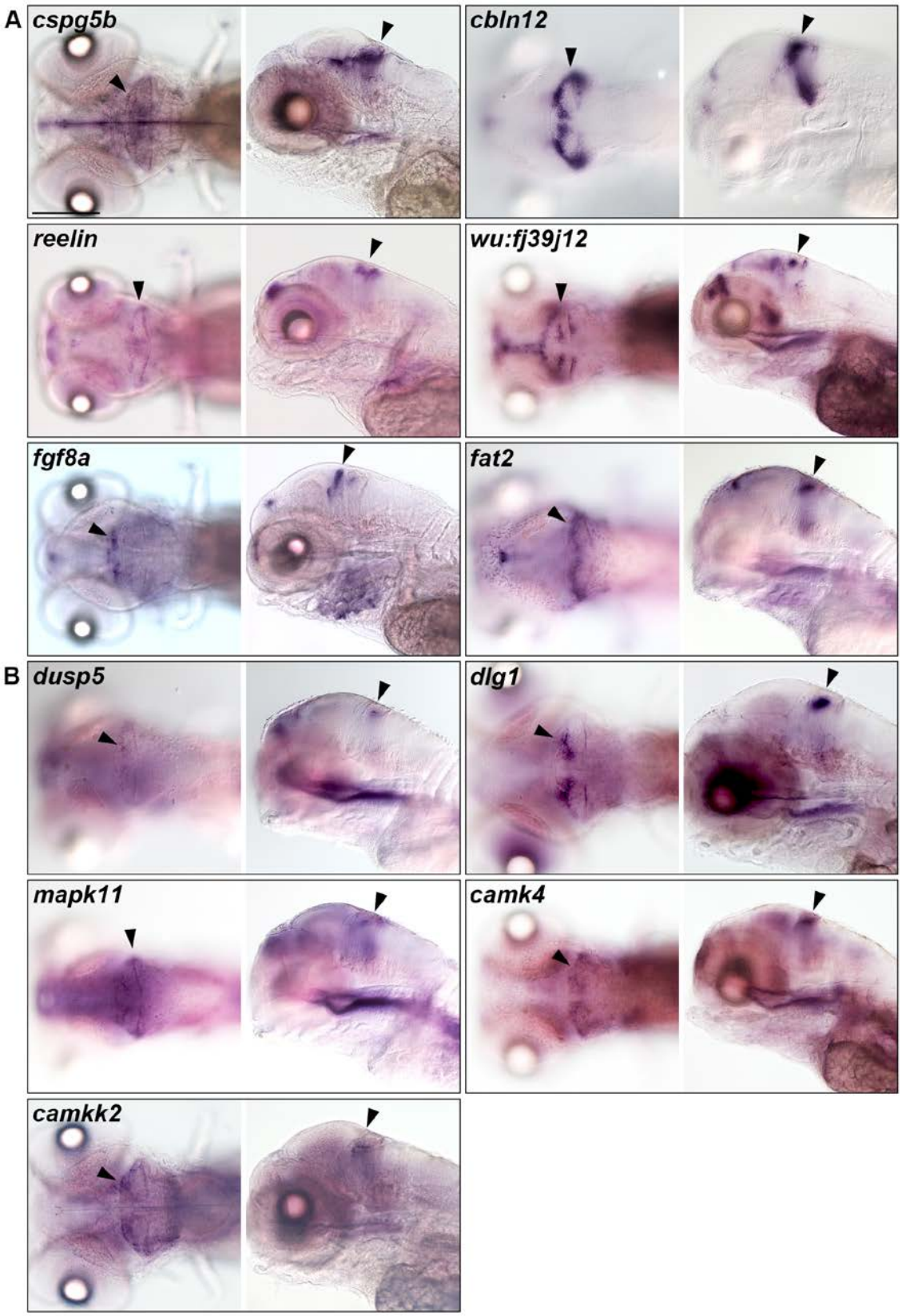

Figure 3. Expression of granule-cell genes at the early larval stage (5 dpf).

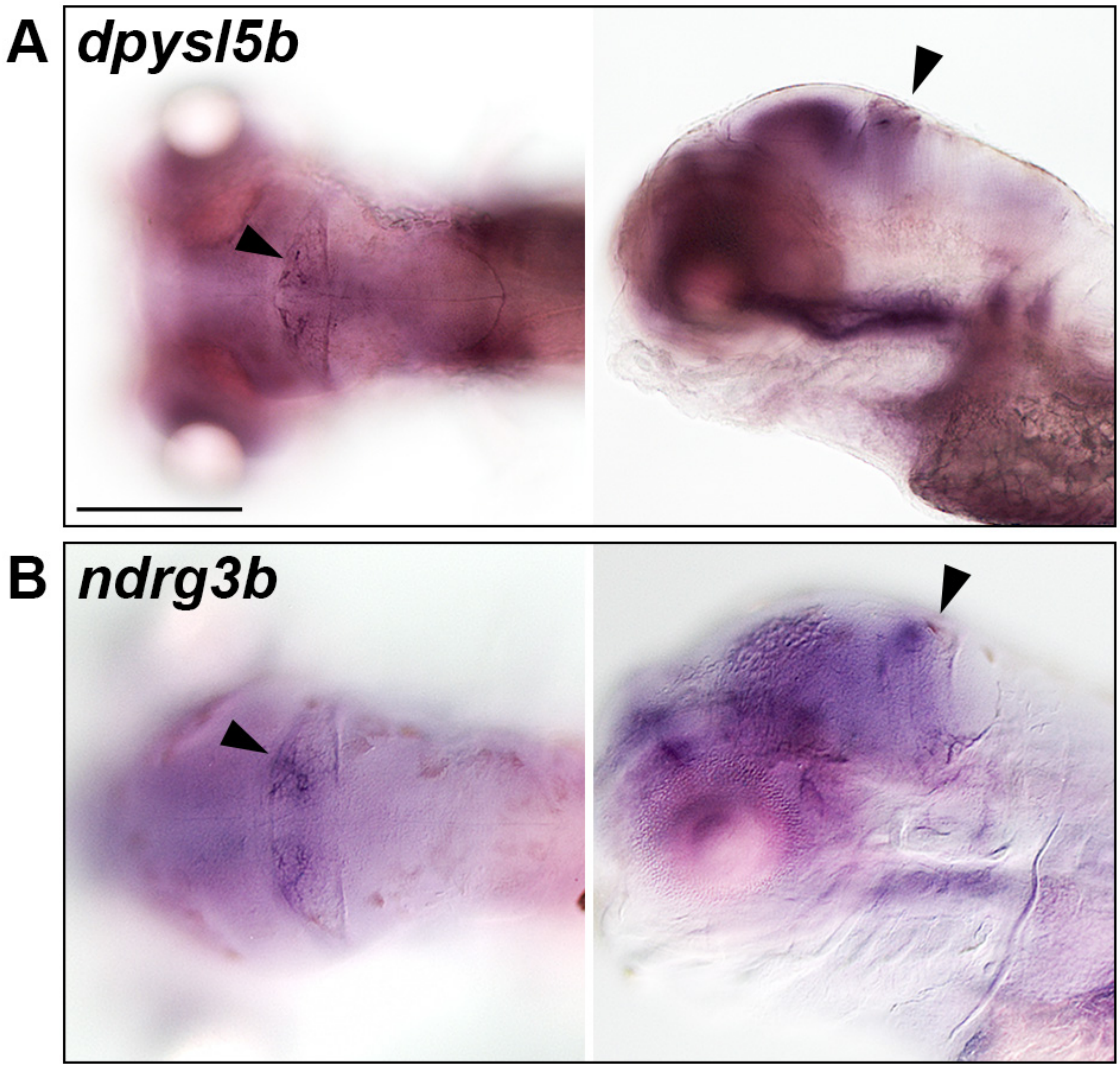

Figure 4. Expression of granule-cell genes at the early larval stage (5 dpf).

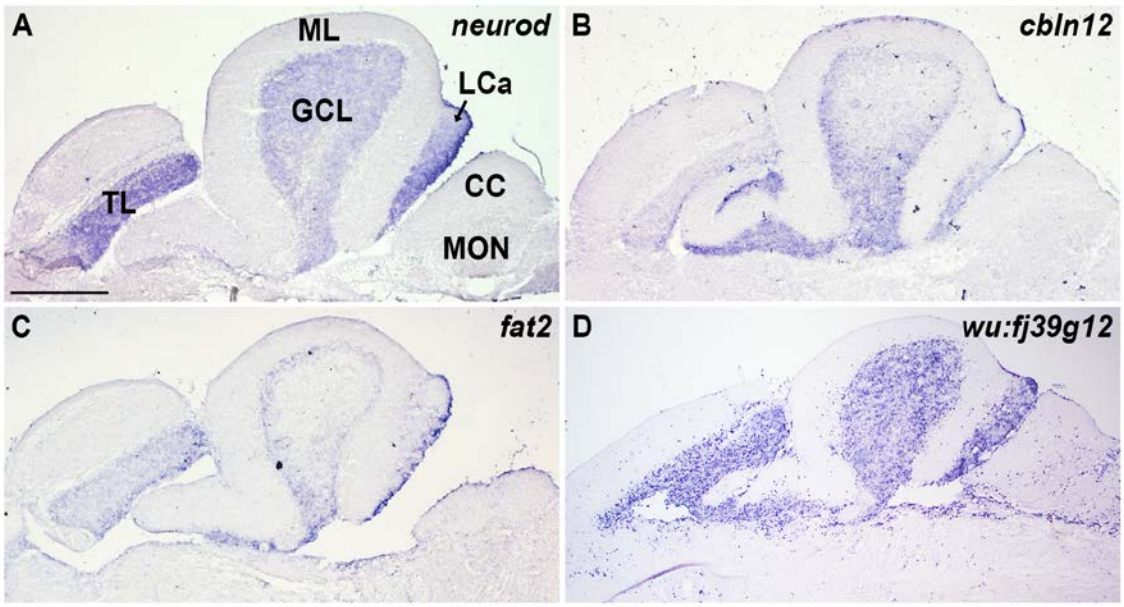

Figure 5. Expression of granule-cell genes in regions of the adult cerebellum.

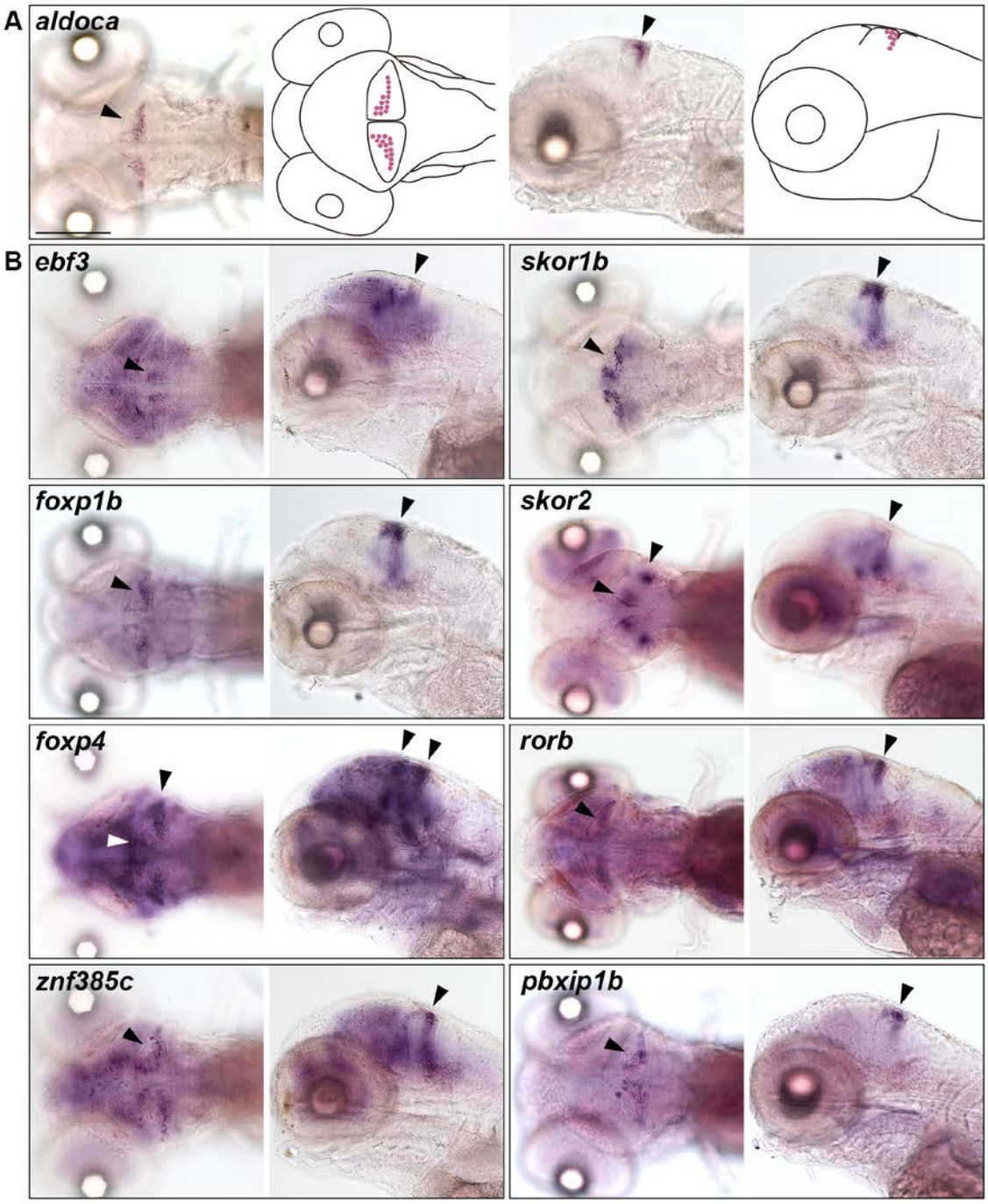

Figure 6. Expression of Purkinje-cell genes at the early larval stage (5 dpf).

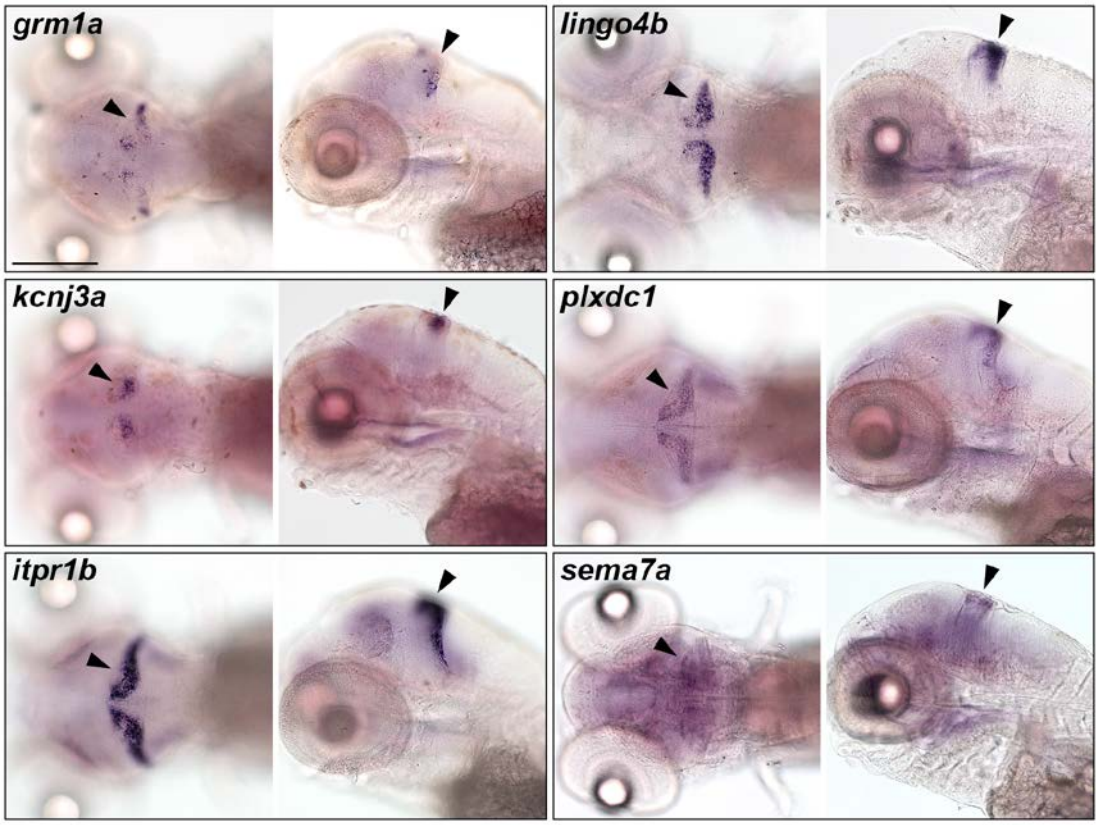

Figure 7. Expression of Purkinje-cell genes at the early larval stage (5 dpf).

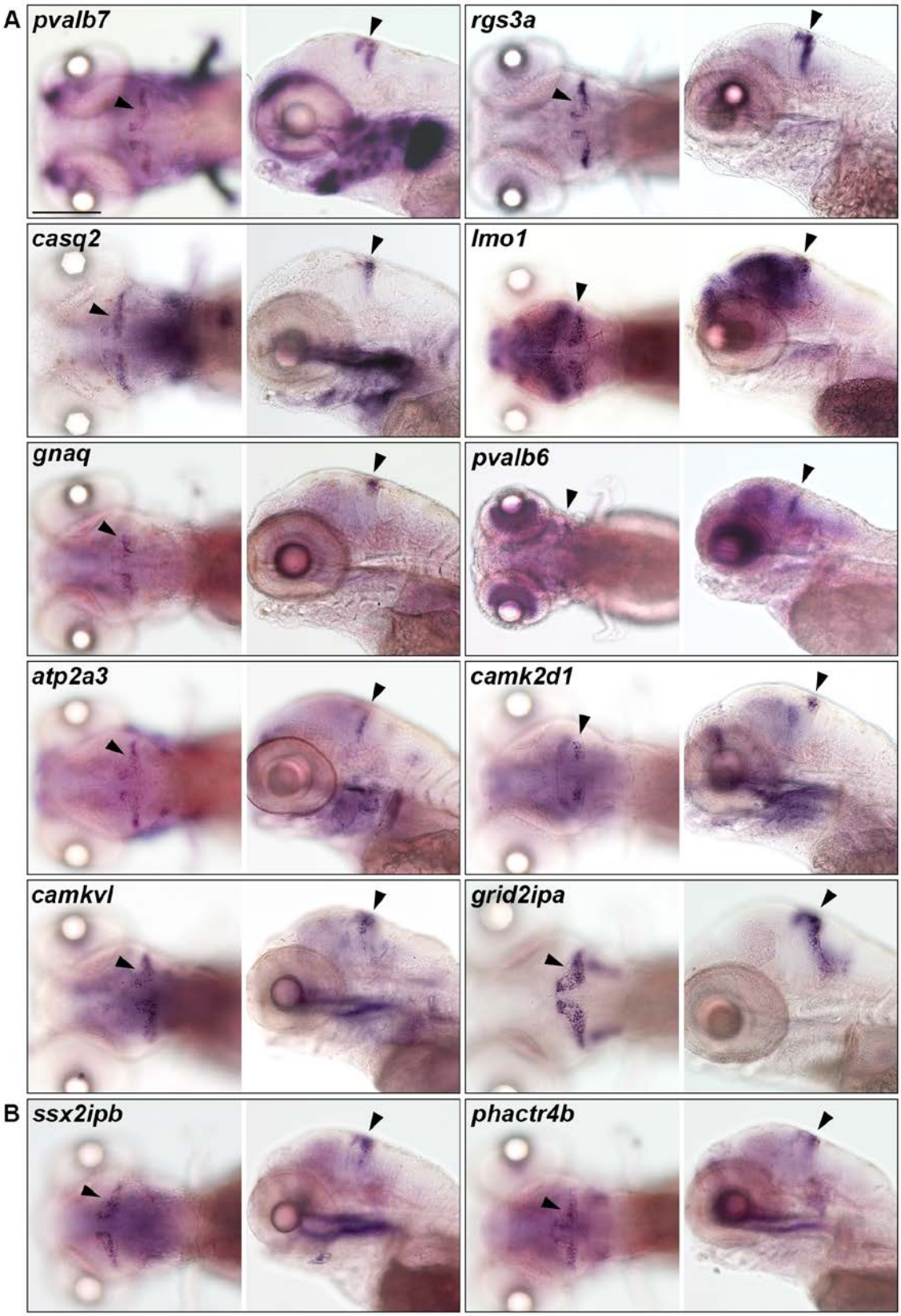

Figure 8. Expression of Purkinje-cell genes at the early larval stage (5 dpf).

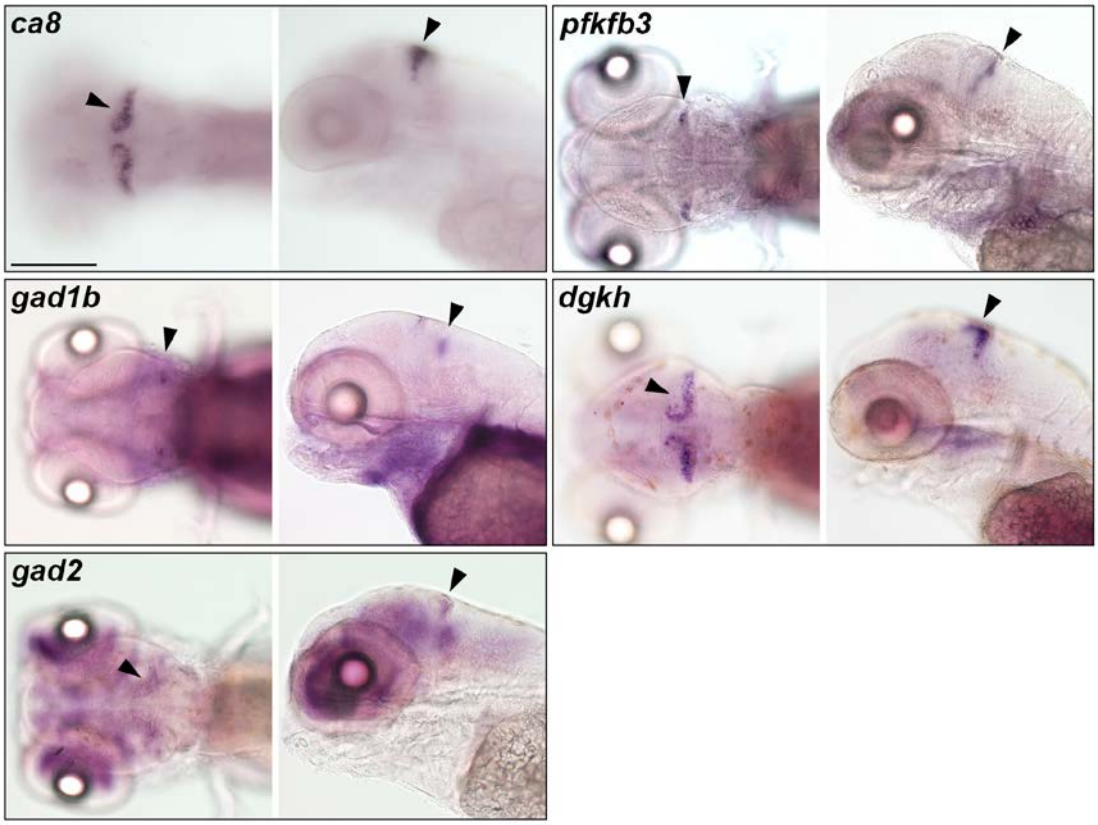

Figure 9. Expression of Purkinje-cell genes at the early larval stage (5 dpf).

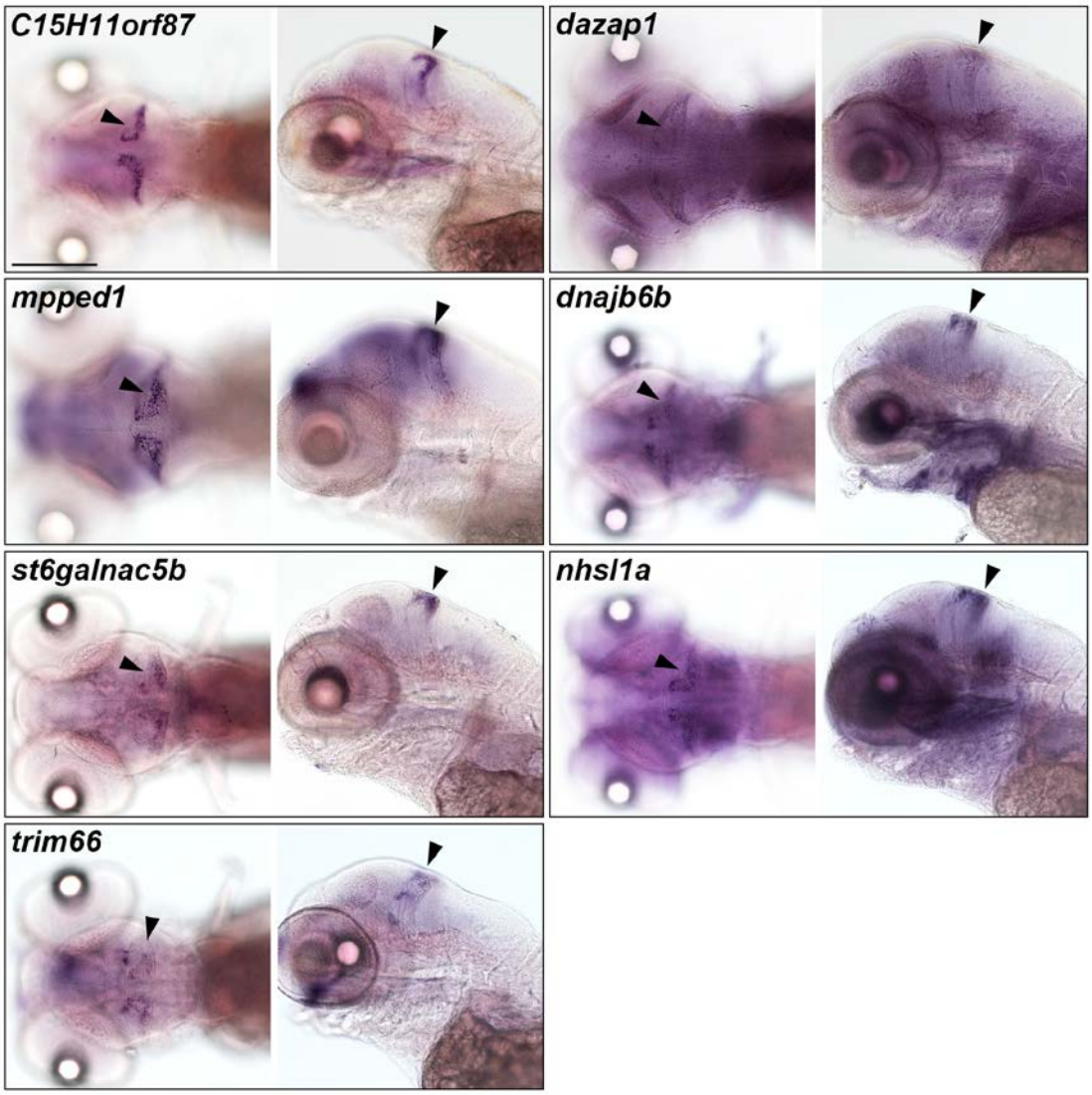

Figure 10. Expression of Purkinje-cell genes at the early larval stage (5 dpf).

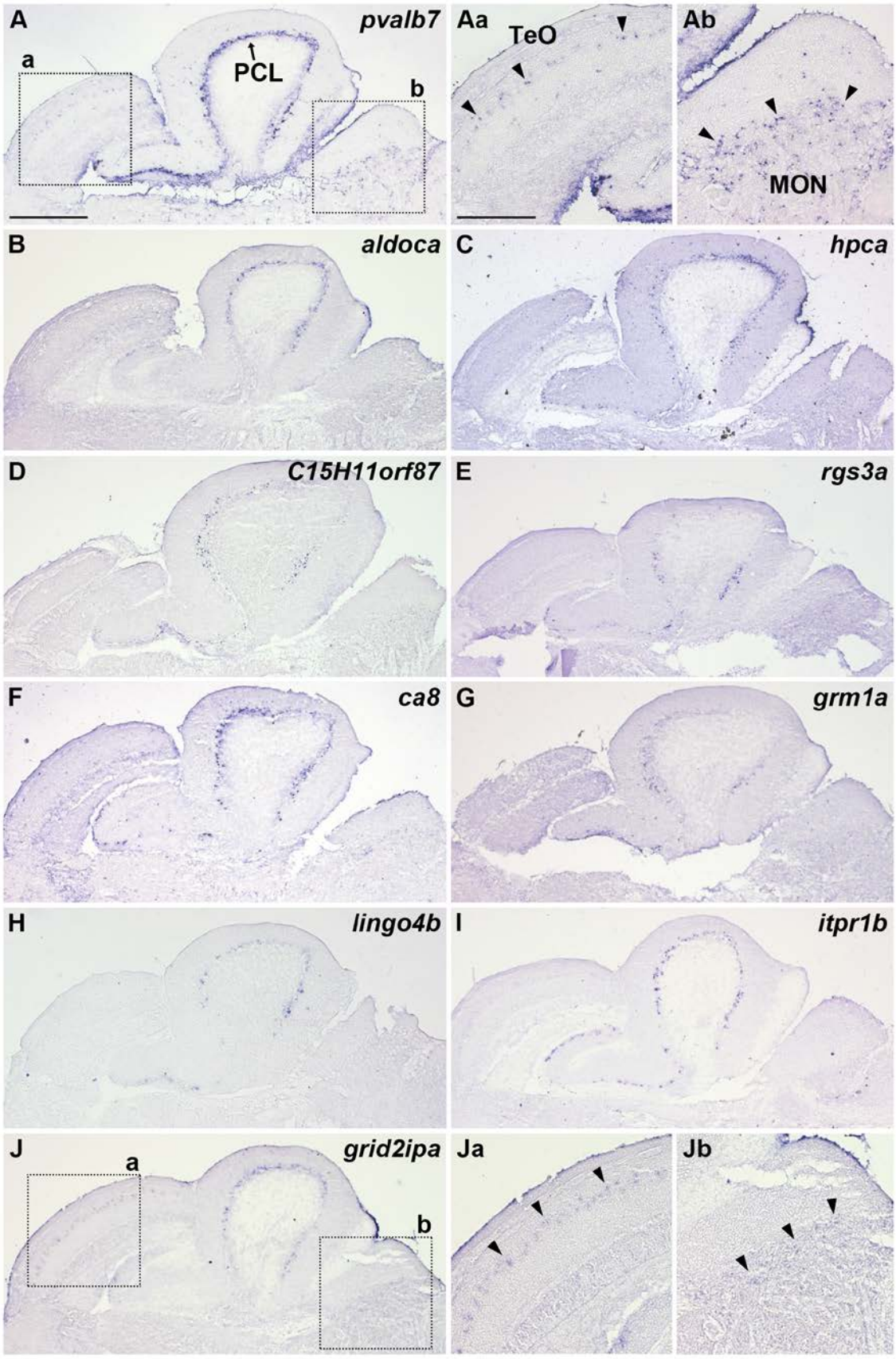

Figure 11. Expression of Purkinje-cell genes in the adult cerebellum and cerebellum-like structures.

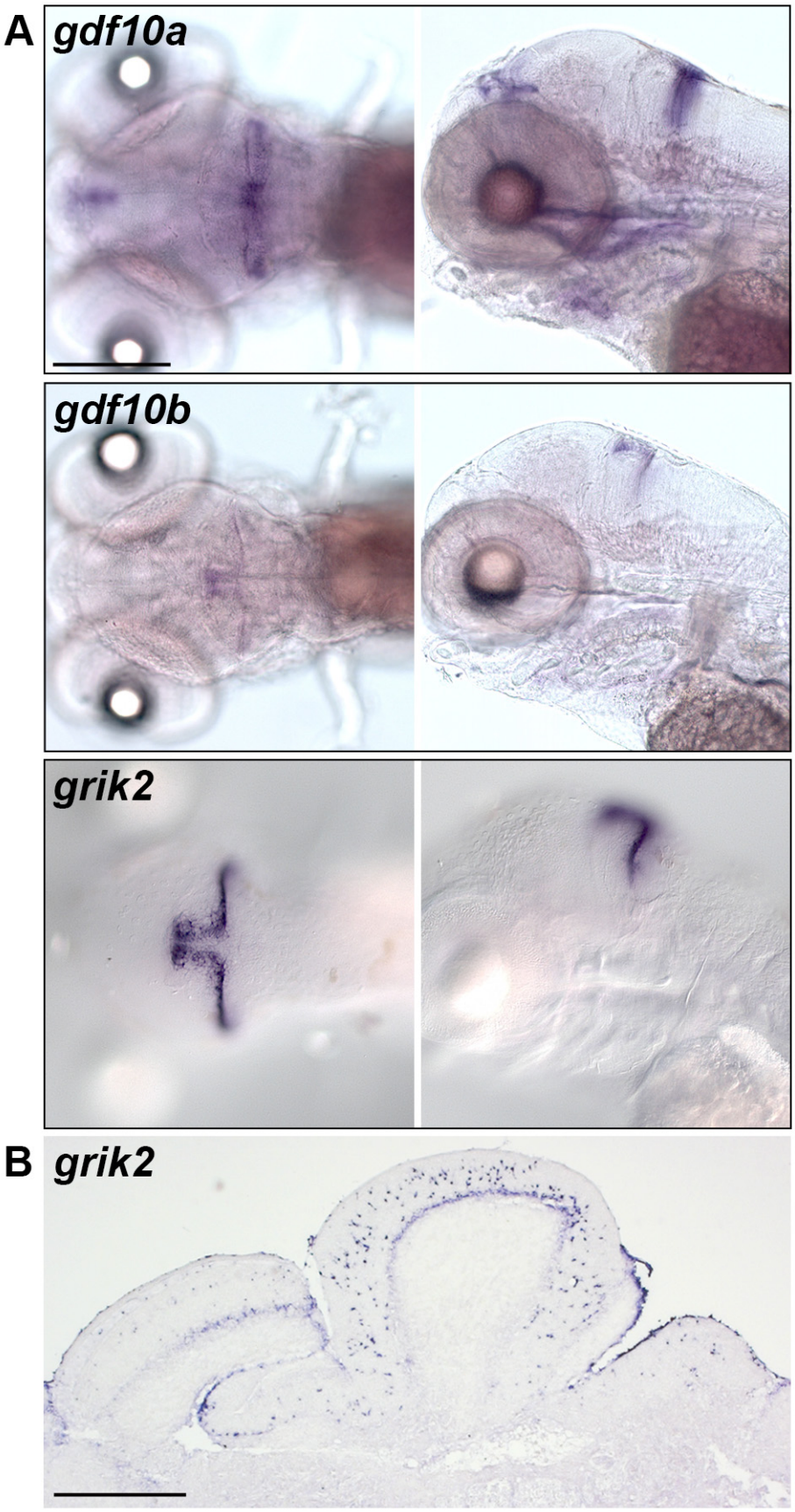

Figure 12. Expression of Bergmann glial genes at 5 dpf and in the adult brain.